36. Ono Y, Fukuhara N, Yoshie O. Transcriptional activity of TAL1 in T cell acute lymphoblastic leukemia (T-ALL) requires RBTN1 or -2 and induces TALLA1, a highly specific tumor marker of T-ALL. J Biol Chem 1997;272:4576–81.
37. Aplan PD, Jones CA, Chervinsky DS, et al. An scl gene product lacking the transactivation domain induces bony abnormalities and cooperates with to generate T-cell malignancies in transgenic mice. EMBO J 1997;16:2408–19.
38. Eggert A, Grotzer MA, Ikegaki N, Liu XG, Evans AE, Brodeur GM. Expression of the neurotrophin receptor TrkA down-regulates expression and function of angiogenic stimulators in SH-SY5Y neuroblastoma cells. Cancer Res 2002;62:1802–8.
39. Ono Y, Fukuhara N, Yoshie O. TAL1 and LIM-only proteins synergistically induce retinaldehyde dehydrogenase 2 expression in T-cell acute lymphoblastic leukemia by acting as cofactors for GATA3. Mol Cell Biol 1998;18:6939–50.
40. Lutz W, Stohr M, Schurmann J, Wenzel A, Lohr A, Schwab M. Conditional expression of N-*myc* in human neuroblastoma cells increases expression of α-prothymosin and ornithine decarboxylase and accelerates progression into S-phase early after mitogenic stimulation of quiescent cells. Oncogene 1996;13:803–12.
41. Schuldiner O, Benvenisty N. A DNA microarray screen for genes involved in c-MYC and N-MYC oncogenesis in human tumors. Oncogene 2001;20:4984–94.
42. Shohet JM, Hicks MJ, Plon SE, et al. Minichromosome maintenance protein MCM7 is a direct target of the MYCN transcription factor in neuroblastoma. Cancer Res 2002;62:1123–8.

VOLUME 23 · NUMBER 22 · AUGUST 1 2005

JOURNAL OF CLINICAL ONCOLOGY

ORIGINAL REPORT

Prediction of *MYCN* Amplification in Neuroblastoma Using Serum DNA and Real-Time Quantitative Polymerase Chain Reaction

Takahiro Gotoh, Hajime Hosoi, Tomoko Iehara, Yasumichi Kuwahara, Shinya Osone, Kunihiko Tsuchiya, Miki Ohira, Akira Nakagawara, Hiroshi Kuroda, and Tohru Sugimoto

From the Department of Pediatrics, Kyoto Prefectural University of Medicine, Graduate School of Medical Science, Kyoto; and Division of Biochemistry, Chiba Cancer Center Research Institute, Chiba, Japan.

Submitted October 6, 2004; accepted April 13, 2005.

Supported by Grants-in-Aid for Scientific Research grant Nos. 15659248, 15659249, and 14370250 from the Ministry of Education, Culture, Sports, Science and Technology of Japan.

Authors' disclosures of potential conflicts of interest are found at the end of this article.

Address reprint requests to Takahiro Gotoh, MD, PhD, Department of Pediatrics, Kyoto Prefectural University of Medicine, Graduate School of Medical Science, Kamigyo-ku, Kyoto 602-8566, Japan; e-mail: takahiro_email:@yahoo.co.jp.

0732-183X/05/2322-5205/$20.00

DOI: 10.1200/JCO.2005.02.014

ABSTRACT

Purpose

MYCN amplification (MNA) indicates a poor prognosis in neuroblastoma (NB) and is routinely assayed for therapy stratification. We aimed to develop a diagnostic tool to predict *MYCN* status using serum DNA, which, in cancer patients, predominantly originates from tumor-released DNA.

Patients and Methods

Using DNA-based real-time quantitative polymerase chain reaction, we simultaneously quantified *MYCN* (2p24) and a reference gene, *NAGK* (2p12), and evaluated *MYCN* copy number as an *MYCN/NAGK* (*M/N*) ratio in 87 NB patients whose *MYCN* status had been determined by Southern blotting. Of these patients, 17 had *MYCN*-amplified NB, and 70 had nonamplified NB.

Results

The serum *M/N* ratio in the MNA group (median, 199.32; range, 17.1 to 901.6; 99% CI, 107.0 to 528.7) was significantly ($P < .001$) higher than the ratio in the non-MNA group (median, 0.87; range, 0.25 to 4.6; 99% CI, 0.82 to 1.26; Mann-Whitney *U* test). The sensitivity and specificity of the serum *M/N* ratio as a diagnostic test were both 100% when the serum *M/N* ratio cutoff was set at 10.0. Among six MNA patients whose clinical courses were followed, the serum ratios decreased to the normal range in the patients in remission (n = 3), whereas the ratios increased to high levels in the patients who relapsed (n = 2) or failed to achieve remission (n = 1).

Conclusion

Measurement of the serum *M/N* ratio seems to be a promising method for accurately assessing *MYCN* status in NB, although a larger set of patients needs to be examined to confirm this result.

J Clin Oncol 23:5205-5210. © 2005 by American Society of Clinical Oncology

INTRODUCTION

Neuroblastoma (NB) is the most common extracranial solid tumor in children and is characterized by a wide range of clinical behaviors, from spontaneous regression to rapid progression with a fatal outcome. The clinical heterogeneity has been reported to be associated with a variety of biologic features of NB. One such aberration, *MYCN* amplification (MNA; ie, creation of multiple copies of the *MYCN* gene in the nuclei of tumor cells), is strongly associated with rapid tumor progression and a poor outcome. MNA is detected in 4% of patients in the early stages of NB, 8% of patients in stage 4S, and approximately 30% of patients in advanced stages. Currently, assessment of *MYCN* status is essential for determining therapy stratification in NB.[1-6] Having rapid access to selected biologic data for each tumor has become increasingly important in

routing patients to appropriate therapies. Several years ago, fluorescence in situ hybridization (FISH) replaced Southern blotting as the most accurate and timely way of evaluating tumors for MNA. Using FISH, the turnaround time for results was shortened from weeks to days, making its use in clinical trials realistic.

In this study, we describe a real-time polymerase chain reaction (PCR) method for evaluating *MYCN* status that shortens the turnaround for results to just a few hours. Furthermore, to facilitate the evaluation of *MYCN* status of tumors, we used serum DNA for the PCR template, which, in cancer patients, predominantly consists of tumor-released DNA.[7] Quantification of serum DNA has also been proposed as a screening tool for early detection of lung cancer.[8] Several groups were able to detect tumor-related aberrations, such as loss of heterozygosity and mutations in the *p53* gene, using the serum DNA of patients with a malignant tumor.[9-11]

Recently, Combaret et al[12] reported that high levels of *MYCN* DNA were present in the peripheral blood of patients with *MYCN*-amplified NB. However, they evaluated serum *MYCN* (2p24) dosage based on PCR without a reference gene, so their assay could be influenced by the quality of the template DNA or a numerical change of chromosome 2. To avoid these problems, we used DNA-based real-time quantitative PCR and a single copy reference gene, the *N-acetylglucosamine kinase* gene (*NAGK*; 2p12), so that *MYCN* copy number per chromosome 2 could be evaluated as the *MYCN/NAGK* (*M/N*) ratio. *NAGK* was chosen because it is on the same chromosome as *MYCN* but sufficiently distant from the region spanned by the *MYCN* amplicon (2p12 *v* 2p24)[13] that a numerical change in chromosome 2 would not affect the *M/N* ratio. The diagnostic performance of the test was evaluated in patients with an NB whose *MYCN* status had been determined by Southern blotting.

PATIENTS AND METHODS

Subjects

Eighty-seven patients diagnosed with NB at the Hospital of the Kyoto Prefectural University of Medicine and Chiba Cancer Center Research Institute were enrolled onto this study with the informed consent of their parents. The studies were conducted under research protocols approved by each institutional review board. At the time of diagnosis, 44 patients were younger than 1 year, and 43 were between 1 and 13 years of age. Seventeen of the patients had MNA, and 70 patients did not have MNA, as determined by Southern blotting. According to the International Neuroblastoma Staging System,[4] the 17 children with MNA included one patient each in stage 1 and 2B, two in stage 3, and 13 in stage 4, whereas the 70 children without MNA included 22 in stage 1, 18 in stage 2A and 2B, five in stage 4S, seven in stage 3, and 18 in stage 4.

Twelve of the 17 patients with MNA and 33 of the 70 nonamplified patients were also analyzed by dual-color FISH technique, as previously described,[14] using an *MYCN* probe (pNb101) and a chromosome 2 centromere probe (D2Z). FISH results of these patients were consistent with the Southern blotting results, although three of the patients who were diagnosed as non-MNA by Southern blotting were found to have one to four extra copies of the *MYCN* gene relative to the chromosome 2 centromere number by FISH. This low level of amplification has been defined as *MYCN* gain, which is an intermediate stage between MNA and non-MNA.[15] Because the prognostic significance of *MYCN* gain is still unclear, these patients were classified as non-MNA according to the Southern blotting results.

Sample Preparation

Tumor specimens were surgically resected and immediately stored at −80°C. Peripheral blood was obtained from each patient before any therapy and surgery. To avoid contamination of serum DNA by the DNA from WBCs, we prepared serum exclusively from the liquid fraction of clotted blood after centrifugation at 1,000 × *g* for 10 minutes and stored it at −20°C until DNA extraction.

DNA Isolation

DNA was extracted from tissues and serum samples by using the QIAmp tissue and blood kits (Qiagen, GmbH, Hilden, Germany), respectively, according to the manufacturer's protocols. For each patient, 200 μL of the stored serum was used for extraction of free DNA.

Real-Time Quantitative PCR

TaqMan PCR was performed using the ABI Prism 5700 Sequence Detection System (Applied Biosystems, Foster City, CA). The PCR mixture contained TaqMan universal PCR master mix (Applied Biosystems), 200 nmol/L of each primer, and 100 nmol/L of fluorogenic probe. The principle of the TaqMan analysis has been described previously in detail.[16-18] In addition to the *MYCN* sequence, *NAGK* (GenBank accession No. NM 017567) located at 2p12 was simultaneously measured as a single-copy reference gene. The sequence of primers and the TaqMan probe used for *MYCN* and *NAGK* are as follows: *MYCN* forward, 5′-GTGCTCTCCAATTCTCGCCT-3′; *MYCN* reverse, 5′-GATGGCCTAGAGGAGGGCT-3′; *MYCN* probe, 5′-FAM-CACTAAAGTTCCTTCCACCCTCTCCT-TAMRA-3′; *NAGK* forward, 5′-TGGGCAGACACATCGTAGCA-3′; *NAGK* reverse, 5′-CACCTTCACTCCCACCTCAAC-3′; and *NAGK* probe, 5′-VIC-TGTTGCCCGAGATTGACCCGGT-TAMRA-3′. All PCR reactions were performed with one cycle of 95°C for 5 minutes, followed by PCR amplification with 50 cycles of 95°C for 15 seconds and 60°C for 1 minute. Standard curves were constructed in each PCR run with four-fold serial dilutions containing 20, 5, 1.25, 0.3125, and 0.078125 ng/μL of a healthy donor's DNA in addition to 20 ng/μL of salmon sperm DNA, and the dosages of the target genes in each sample were interpolated using these standard curves. The *MYCN* copy number of a sample of DNA was determined by the ratio of the *MYCN* dosage to the *NAGK* dosage (*M/N* ratio). Copy numbers were expressed as the average of two measurements.

Effect of WBC Contamination

To assess the effect of WBC contamination in serum samples on the serum *M/N* ratio, we measured the serum *M/N* ratio using DNA extracted from a series of WBC-contaminated serum samples. The samples were prepared by adding 0, 1×10, 1×10^2, 1×10^3, 1×10^4, and 1×10^5 of WBCs from a healthy donor to 200 μL of serum from a *MYCN*-amplified patient.

Statistical Methods

The difference in the serum *M/N* ratio between the MNA and non-MNA groups was assessed using the Mann-Whitney *U* test. $P < .05$ was judged as significant.

Serum M/N Ratio As a Predictor of MYCN Status of Tumor

Serum *M/N* ratios could be determined in approximately 4 hours by real-time quantitative PCR. Figure 1 shows the distribution of the serum *M/N* ratio in the MNA and non-MNA groups at the time of diagnosis. The serum *M/N* ratio in the MNA group (n = 17; median, 199.32; range, 17.1 to 901.6; 99% CI, 107.0 to 528.7) was significantly ($P < .001$) higher than the ratio in the non-MNA group (n = 70; median, 0.87; range, 0.25 to 4.6; 99% CI, 0.82 to 1.26). In fact, there was no overlap between the two groups in the limited number of patients examined in this study. As a cutoff for the serum *M/N* ratio to distinguish between MNA and non-MNA patients, we empirically chose a value of 10, which was in the middle of the two ranges. With this value, the sensitivity and specificity of the serum *M/N* ratio as a diagnostic test to distinguish patients with MNA from those without MNA were both 100% for our limited number of patients. That is, the serum *M/N* ratio was in complete agreement with the Southern blotting results. The positive and negative predictive values were 100%. The serum *M/N* ratios were also consistent with results obtained by FISH for 45 of the patients (FISH analyses were performed in 12 of the 17 MNA patients and in 33 of the 70 nonamplified patients). Three of the patients who had one to four extra copies of the *MYCN* gene relative to chromosome 2 centromere number, as determined by FISH, also had slightly elevated serum *M/N* ratios (2.5, 3.3, and 4.6).

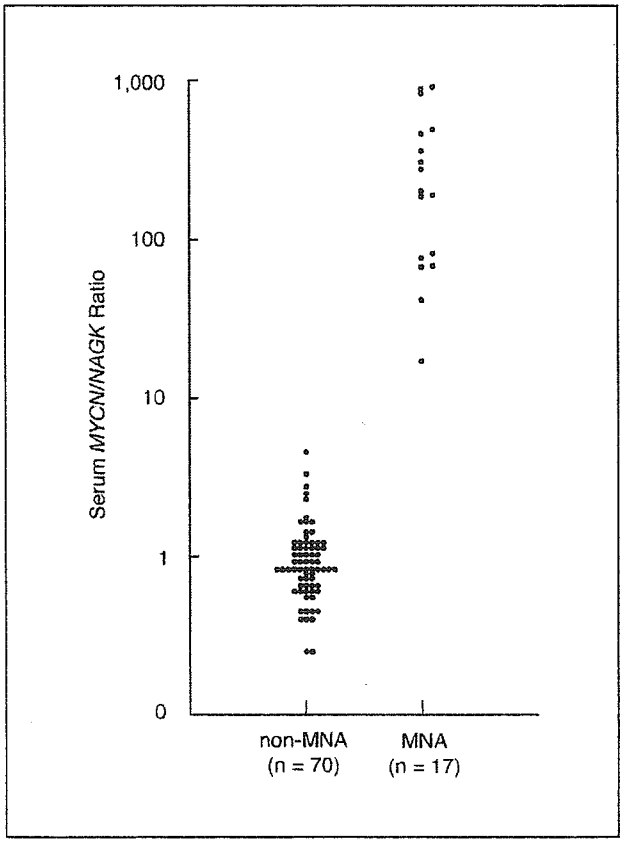

Fig 1. A scatter plot of serum *MYCN/NAGK* ratio in patients with *MYCN*-amplified (MNA) and nonamplified (non-MNA) neuroblastoma. The serum *MYCN/NAGK* ratio was significantly ($P < .001$) higher in the MNA group (median, 199.32; range, 17.1 to 901.6; 99% CI, 107.0 to 528.7) than in the non-MNA group (median, 0.87; range, 0.25 to 4.6; 99% CI, 0.82 to 1.26; Mann-Whitney *U* test).

Change in Serum M/N Ratio Levels During Follow-Up

To evaluate whether an increase in the serum *M/N* ratio can be used as an indicator of relapse, we measured serum *M/N* ratios at several points in the clinical courses of six patients with MNA (Fig 2). In three patients who were in complete remission (patients 1, 2, and 3), the serum *M/N* ratios decreased to the normal range and were consistently low. In contrast, in one patient who failed to achieve remission (patient 4), the serum *M/N* ratio did not decrease to the normal range and remained at a high level until his death. In the other patients who experienced recurrence after remission (patients 5 and 6), the serum *M/N* ratio first decreased to the normal range and then increased beyond the cutoff value by the time of diagnosis.

Effect of WBC Contamination on Serum M/N Ratio

We found that a high serum *M/N* ratio could be masked by the presence of WBC. The *M/N* ratio of serum from an *MYCN*-amplified patient decreased with increasing WBC contamination (Fig 3). When 200 μL of serum was contaminated with 1×10^5 of WBC, corresponding to approximately one fortieth of the WBC concentration in normal whole blood, the serum *M/N* ratio decreased below the cutoff level.

DISCUSSION

Serum markers, such as ferritin,[19] lactic dehydrogenase,[20] and neuron-specific enolase,[21] have been proposed as prognostic markers of NB, although they have shown little prognostic value. Recently, elevated levels of plasma midkine have been reported to correlate with a poor prognosis. However, the significance of this finding is controversial because plasma midkine levels are highest in stage 4S patients.[22] Therefore, a noninvasive assay of tumor-related

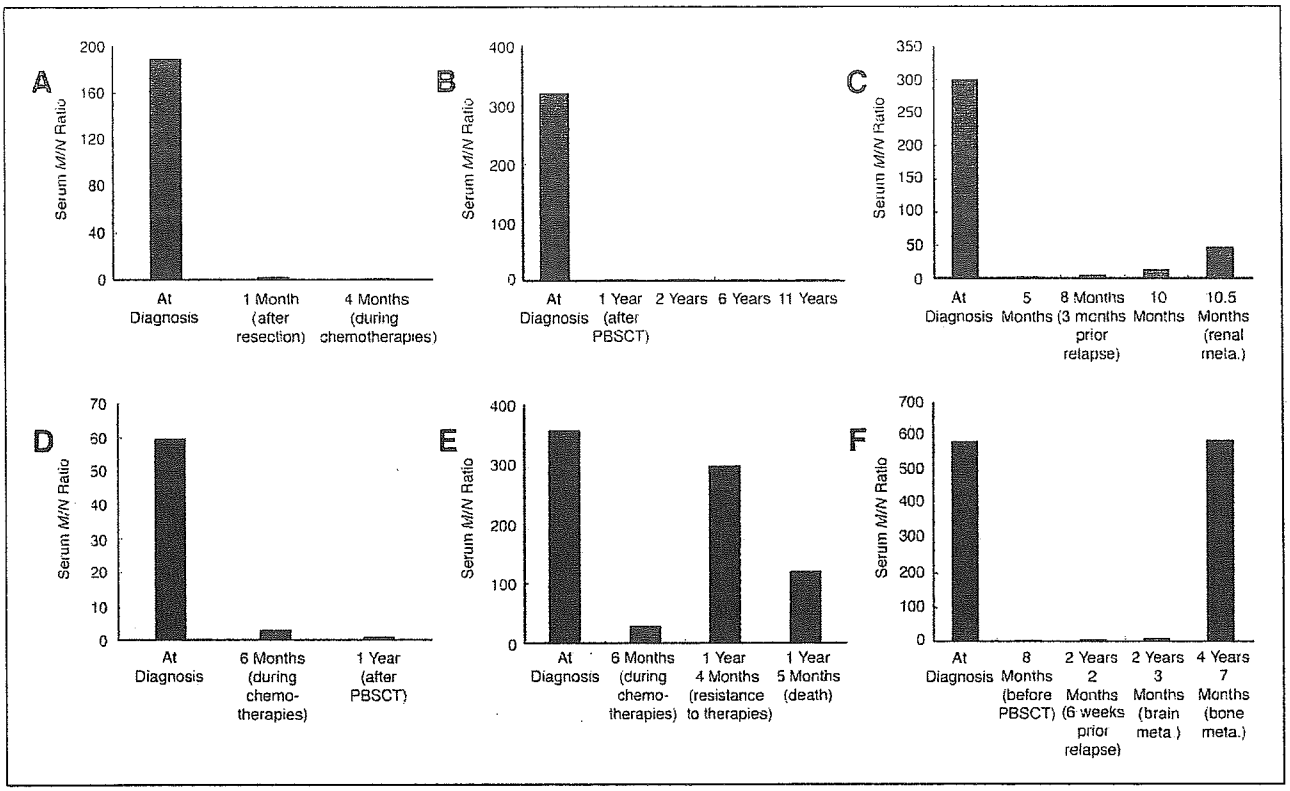

Fig 2. Changes in serum *MYCN/NAGK* (*M/N*) ratio levels of six patients with *MYCN* amplification during follow-up. PBSCT, peripheral-blood stem-cell transfusion; meta., metastasis. (A) Patient 1; (B) patient 3; (C) patient 5; (D) patient 2; (E) patient 4; (F) patient 6.

genetic aberrations using serum DNA is desirable for the assessment of prognosis and therapy stratification at the time of diagnosis. Among the tumor-related genetic aberrations detected in NB, MNA was of greatest interest to us because of its significant prognostic value.

By using DNA-based real-time quantitative PCR with a single-copy reference gene, we have demonstrated that the *M/N* ratio in serum DNA is a valuable diagnostic tool to discriminate MNA patients from non-MNA patients. The serum *M/N* ratio in the MNA group was significantly higher than the ratio in the non-MNA group, without an overlap. The highest sensitivity (100%), highest specificity (100%), highest positive predictive value (100%), and highest negative predictive value (100%) were obtained with a serum *M/N* ratio cutoff value of 10.0. Furthermore, we found an elevated level of the serum *M/N* ratio in a stage 1 patient and a stage 2B patient with MNA (188.7 and 901.6, respectively), even though the tumor was localized in these patients. This suggests that tumors could release a significant amount of genomic DNA into the systemic circulation even at an early stage. Furthermore, Sozzi et al[23] reported that the concentration of plasma DNA in 84 lung cancer patients was higher than the concentration in 43 controls, regardless of the tumor stage, and suggested that circulating DNA in peripheral blood was an early event in lung carcinogenesis.

Another clinical benefit of the serum *M/N* assay is that it could be used as a marker to monitor therapeutic efficacy and recurrence after therapies. The serum *M/N* ratio decreased to the normal range in the patients in remission but remained at a high level in the patient who failed to achieve remission. Furthermore, in two patients with recurrence after remission, the serum *M/N* ratio initially decreased to the normal range but then increased beyond the cutoff value by the time of diagnosis. The serum *M/N* ratio did not increase to the initial level as long as the metastasis was localized in the brain, but it did increase to the initial level when the patient later developed a bone metastasis (patient 6). This is noteworthy because it suggests that a brain metastasis releases genomic DNA into the systemic circulation less easily than extracranial tumors. If this is confirmed by examination of additional patients, then it is possible that tumors localized in brain could be overlooked with diagnostic assays based on serum DNA.

A possible pitfall of our serum *M/N* assay is that a high serum *M/N* ratio could be reduced by WBC contamination (Fig 3). This could be a result of dilution of tumor DNA with the WBC DNA, which would be expected to have an *M/N* ratio of 1. Therefore, the importance of removing WBCs from serum should be addressed in diagnostic assays

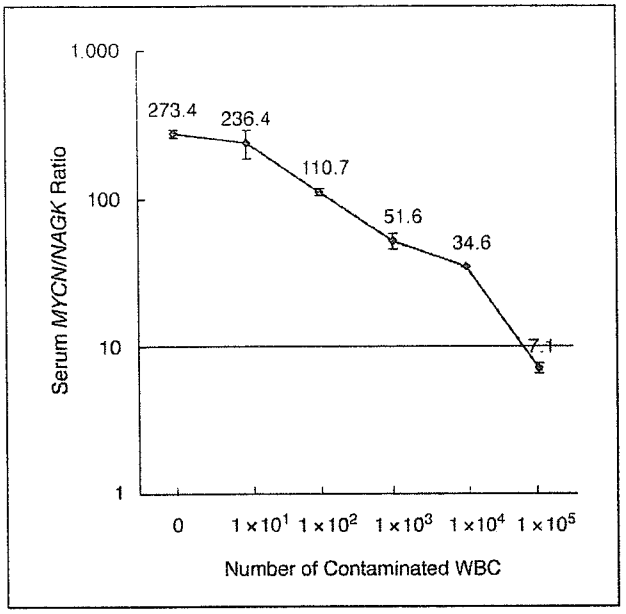

Fig 3. Influence of WBC contamination in serum samples on the serum *MYCN/NAGK* ratio. Data are presented as the mean ± standard deviation of duplicate measurements. The transverse line represents a *MYCN/NAGK* ratio cutoff value of 10.0.

that use serum DNA. For the same reason, a predominance of any nontumor DNA in serum may lower an elevated *M/N* ratio of an *MYCN*-amplified patient. However, this assay can be accurate on the premise that, in cancer patients, serum DNA predominantly consists of tumor-released DNA.[7] In addition, the use of serum DNA as a diagnostic tool in lung cancer patients has resulted in a diversity of findings, suggesting that these differences likely reflect variations in the manner in which the blood specimens were collected and handled and variations in the methods by which the assay were conducted.[24] Therefore, it is necessary to standardize the serum collection procedure to ensure that different laboratories obtain the same result with a given blood sample. An additional high-speed centrifugation step (16,000 × *g* for 5 minutes) was found to eliminate cellular contamination even after thawing of stored samples.[25] By using the appropriate centrifugation methods, we believe that WBC-free serum can be reliably achieved.

Although a large set of patients needs to be studied to verify the accuracy of this assay and to set an appropriate cutoff, our results are promising and need to be further tested. The advantages of this method are that it takes only 4 hours and much less effort than FISH and Southern blotting, which should make this assay an alternative to these other methods for determining *MYCN* status. A third advantage is that the serum *M/N* ratio seems to be a promising indicator of therapeutic efficacy and relapse in the follow-up of patients with MNA, although more patients need to be examined to confirm its reliability.

Acknowledgment

We thank two anonymous reviewers for helpful comments.

Authors' Disclosures of Potential Conflicts of Interest

The authors indicated no potential conflicts of interest.

REFERENCES

1. Brodeur GM, Seeger RC, Schwab M, et al: Amplification of N-myc in untreated human neuroblastomas correlates with advanced disease stage. Science 224:1121-1124, 1984
2. Seeger RC, Brodeur GM, Sather H, et al: Association of multiple copies of the N-myc oncogene with rapid progression of neuroblastomas. N Engl J Med 313:1111-1116, 1985
3. Brodeur GM, Maris JM, Yamashiro DJ, et al: Biology and genetics of human neuroblastomas. J Pediatr Hematol Oncol 19:93-101, 1997
4. Brodeur GM, Pritchard J, Berthold F, et al: Revisions of the international criteria for neuroblastoma diagnosis, staging and response to treatment. J Clin Oncol 11:1466-1477, 1993
5. Castleberry RP, Prichard J, Ambros P, et al: The International Neuroblastoma Risk Groups (INRG): A preliminary report. Eur J Cancer 33:2113-2116, 1997
6. Shimada H, Ambros IM, Dehner LP, et al: The International Neuroblastoma Pathology Classification System (the Shimada system). Cancer 86:364-372, 1999
7. Shapiro B, Chakrabarty M, Cohn EM, et al: Determination of circulating DNA levels in patients with benign or malignant gastrointestinal disease. Cancer 51:2116-2120, 1983
8. Sozzi G, Conte D, Leon M, et al: Quantification of free circulating DNA as a diagnostic marker in lung cancer. J Clin Oncol 21:3902-3908, 2003
9. Sozzi G, Musso K, Ratcliffe C, et al: Detection of microsatellite alterations in plasma DNA of non-small cell lung cancer patients: A prospect for early diagnosis. Clin Cancer Res 5:2689-2692, 1999
10. Chen X, Bonnefoi H, Diebold-Berger S, et al: Detecting tumor-related alterations in plasma or serum DNA of patients diagnosed with breast cancer. Clin Cancer Res 5:2297-2303, 1999
11. Silva JM, Dominguez G, Garcia JM, et al: Presence of tumor DNA in plasma of breast cancer patients: Clinicopathological correlations. Cancer Res 59:3251-3256, 1999
12. Combaret V, Audoynaud C, Iacono I, et al: Circulating *MYCN* DNA as a tumor-specific marker in neuroblastoma patients. Cancer Res 62:3646-3648, 2002
13. Akiyama K, Kanda N, Yamada M, et al: Megabase-scale analysis of the origin of N-myc amplicons in human neuroblastoma. Nucleic Acids Res 22:187-193, 1994
14. Gotoh T, Sugihara H, Matsumura T, et al: Human neuroblastoma demonstrating clonal evolution in vivo. Genes Chromosomes Cancer 22:42-49, 1998
15. Spitz R, Hero B, Skowron M, et al: *MYCN*-status in neuroblastoma: Characteristics of tumours showing amplification, gain, and non-amplification. Eur J Cancer 40:2753-2759, 2004
16. Gelmini S, Orlando C, Sestini R, et al: Quantitative polymerase chain reaction-based homogeneous assay with fluorogenic probes to measure c-erbB-2 oncogene amplification. Clin Chem 43:752-758, 1997
17. Claudia CR, Maria LB, Gian PT, et al: Real-time quantitative PCR for the measurement of *MYCN* amplification in human neuroblastoma with the TaqMan detection system. Clin Chem 45:1918-1924, 1999
18. Chiang PW, Beer DG, Wei WL, et al: Detection of erbB-2 amplifications in tumors and sera from esophageal carcinoma patients. Clin Cancer Res 5:1381-1386, 1999
19. Hann HWL, Evans AE, Siegel SE, et al: Prognostic importance of serum ferritin in patients with stage III and IV neuroblastoma: The

Children's Cancer Study Group experience. Cancer Res 45:2843-2848, 1985

20. Quinn JJ, Altman AJ, Frantz CN, et al: Serum lactic dehydrogenase, an indicator of tumor activity in neuroblastoma. J Pediatr 97:89-91, 1980

21. Massaron S, Seregni E, Luksch R, et al: Neuron-specific enolase evaluation in patients neuroblastoma. Tumour Biol 19:261-268, 1998

22. Ikematsu S, Nakagawara A, Nakamura Y, et al: Correlation of elevated level of blood midkine with poor prognostic factors of human neuroblastomas. Br J Cancer 88:1522-1526, 2003

23. Sozzi G, Conte D, Mariani L, et al: Analysis of circulating tumor DNA in plasma at diagnosis and during follow-up of lung cancer patients. Cancer Res 61:4675-4678, 2001

24. Bunn PA: Early detection of lung cancer using serum RNA or DNA markers. Ready for "prime time" or for validation? J Clin Oncol 21:3891-3893, 2003

25. Swinkels DW, Wiegerinck E, Steegers EAP, et al: Effect of blood-processing protocols on cell-free DNA quantification in plasma. Clin Chem 49:525-526, 2003

THE JOURNAL OF BIOLOGICAL CHEMISTRY
Vol. 280, No. 17, Issue of April 29, pp. 16665–16675, 2005
Printed in U.S.A.

Identification of Protein Kinase A Catalytic Subunit β as a Novel Binding Partner of p73 and Regulation of p73 Function*

Received for publication, December 20, 2004, and in revised form, January 31, 2005
Published, JBC Papers in Press, February 21, 2005, DOI 10.1074/jbc.M414323200

Takayuki Hanamoto‡§, Toshinori Ozaki‡, Kazushige Furuya‡, Mitsuchika Hosoda‡, Syunji Hayashi‡, Mitsuru Nakanishi‡, Hideki Yamamoto‡, Hironobu Kikuchi‡, Satoru Todo§, and Akira Nakagawara‡¶

From the ‡Division of Biochemistry, Chiba Cancer Center Research Institute, Chiba 260-8717, Japan and the §Department of General Surgery, Hokkaido University School of Medicine, Kita-ku, Sapporo 060-8638, Japan

Post-translational modifications play a crucial role in regulation of the protein stability and pro-apoptotic function of p53 as well as its close relative p73. Using a yeast two-hybrid screening based on the Sos recruitment system, we identified protein kinase A catalytic subunit β (PKA-Cβ) as a novel binding partner of p73. Co-immunoprecipitation and glutathione *S*-transferase pull-down assays revealed that p73α associated with PKA-Cβ in mammalian cells and that their interaction was mediated by both the N- and C-terminal regions of p73α. In contrast, p53 failed to bind to PKA-Cβ. *In vitro* phosphorylation assay demonstrated that glutathione *S*-transferase-p73α-(1–130), which has one putative PKA phosphorylation site, was phosphorylated by PKA. Enforced expression of PKA-Cβ resulted in significant inhibition of the transactivation function and pro-apoptotic activity of p73α, whereas a kinase-deficient mutant of PKA-Cβ had no detectable effect. Consistent with this notion, treatment with H-89 (an ATP analog that functions as a PKA inhibitor) reversed the dibutyryl cAMP-mediated inhibition of p73α. Of particular interest, PKA-Cβ facilitated the intramolecular interaction of p73α, thereby masking the N-terminal transactivation domain with the C-terminal inhibitory domain. Thus, our findings indicate a PKA-Cβ-mediated inhibitory mechanism of p73 function.

p73 has been identified as a structural and functional homolog of the tumor suppressor p53 (1). p53 and p73 share the same domain organization, consisting of an N-terminal transactivation domain, a central sequence-specific DNA-binding domain, and a C-terminal oligomerization domain. As expected, several pieces of evidence suggest that p73 can bind to the p53-responsive element and transactivate an overlapping set of p53 target genes, thus leading to induction of G_1/S cell cycle arrest and apoptosis (1–6). In marked contrast to p53, p73 is expressed as multiple isoforms arising from alternative splicing of the primary p73 transcript (p73α, p73β, p73γ, p73δ, p73ε, p73η, and p73ζ) termed the TA variant (1, 3, 7–9). These alternatively spliced isoforms vary in their C termini and display different transcriptional and biological properties. Additionally, the ΔN variant (ΔNp73α and ΔNp73β), which is generated by alternative promoter utilization, lacks the N-terminal transactivation domain and exhibits dominant-negative behavior toward wild-type p73 as well as p53 (10–12). Recently, we (14) and others (13, 15) demonstrated that p73 directly transactivates the expression of its own negative regulator (ΔNp73), creating an autoregulatory feedback loop in which both the activity of p73 and the expression of ΔNp73 are regulated. Thus, the pro-apoptotic activity of p73 is determined by the relative expression levels of its TAp73 and dominant-negative ΔNp73 variants in cells.

In sharp contrast to p53, it was initially reported that p73 was not induced by DNA damage (1). However, recent studies demonstrated that, in response to a subset of DNA-damaging agents, p73 is positively regulated by multiple post-translational modifications, including phosphorylation and acetylation. During cisplatin-mediated apoptosis, phosphorylation of p73 at Tyr-99 by the non-receptor tyrosine kinase c-Abl results in an increase in its stability and pro-apoptotic activity (16–18). In addition to c-Abl, the protein kinase Cδ catalytic fragment has the ability to phosphorylate p73 at Ser-289 and contributes to the accumulation of p73 during the apoptotic response to cisplatin treatment (19). It is worth noting that the physical and functional interaction between c-Abl and protein kinase Cδ leads to the cross-activation of their kinase functions (20, 21). Furthermore, the enzymatic activity of Chk1 (checkpoint kinase-1) is enhanced in response to DNA damage (22–24), and Chk1 has the ability to phosphorylate p73 at Ser-47 upon DNA damage, thereby enhancing its transactivation ability and pro-apoptotic activity without affecting the level of total p73 protein, whereas Chk2 has no detectable effect on p73 (25). Alternatively, Zeng *et al.* (26) found that the acetyltransferase p300/CBP (cAMP-responsive element-binding protein-binding protein) interacts with the N-terminal region of p73 and stimulates p73-mediated transcriptional activation and apoptosis. Recently, Costanzo *et al.* (27) reported that doxorubicin treatment induces the p300-mediated acetylation of p73 at Lys-321, Lys-327, and Lys-331 in a c-Abl-dependent manner, which is associated with the efficient recruitment of p73 to the promoter of the apoptotic target gene *p53AIP1*. Additionally, it has been shown that p300-mediated acetylation of p73 results in its significant stabilization in a prolyl isomerase Pin1-dependent manner (28).

To identify cellular protein(s) that could interact with full-length p73α and regulate its function, we screened a human fetal brain cDNA library using a yeast two-hybrid method

* This work was supported in part by a grant-in-aid from the Ministry of Health, Labor, and Welfare for Third Term Comprehensive Control Research for Cancer; a grant-in-aid for scientific research on priority areas from the Ministry of Education, Culture, Sports, Science, and Technology of Japan; and a grant-in-aid for scientific research from the Japan Society for the Promotion of Science. The costs of publication of this article were defrayed in part by the payment of page charges. This article must therefore be hereby marked "*advertisement*" in accordance with 18 U.S.C. Section 1734 solely to indicate this fact.

¶ To whom correspondence should be addressed: Div. of Biochemistry, Chiba Cancer Center Research Inst., 666-2 Nitona, Chuoh-ku, Chiba 260-8717, Japan. Tel.: 81-43-264-5431; Fax: 81-43-265-4459; E-mail: akiranak@chiba-cc.jp.

based on the Sos recruitment system. We report here that protein kinase A catalytic subunit β (PKA-Cβ)[1] bound to p73α in cells, but not to p53, and that their interaction was mediated by the N- and C-terminal regions of p73α. *In vitro* kinase assays revealed that the catalytic subunit of PKA phosphorylated p73α. PKA-Cβ inhibited the p73α-mediated transcriptional activation of the $p21^{WAF1}$ and *Bax* promoters and p73α-dependent apoptosis in response to camptothecin. On the other hand, the kinase-deficient mutant of PKA-Cβ had little effect on p73α. Of note, we found that PKA-Cβ facilitated the intramolecular interaction of p73α. Our results strongly suggest the PKA-Cβ-mediated phosphorylation and intramolecular interaction of p73 to be a novel inhibitory mechanism of p73 function.

EXPERIMENTAL PROCEDURES

Cell Culture and Cell Lines—SV40-transformed African green monkey kidney cells (COS-7) were grown in Dulbecco's modified Eagle's medium supplemented with 10% heat-incubated fetal bovine serum (Invitrogen), 100 IU/ml penicillin, and 100 μg/ml streptomycin. p53-deficient human lung carcinoma H1299 cells were maintained in RPMI 1640 medium supplemented with 10% heat-incubated fetal bovine serum and antibiotic mixture. The cells were cultured at 37 °C in a water-saturated atmosphere of 95% air and 5% CO_2.

Transient Transfection—COS-7 cells grown to 50–70% confluence in 60-mm dishes were transfected with the indicated expression plasmids using FuGENE 6 transfection reagent (Roche Applied Science) following the protocol recommended by the manufacturer. H1299 cells transfection was performed using Lipofectamine 2000 transfection reagent (Invitrogen) according to the manufacturer's instructions.

Yeast Two-hybrid Screening—The CytoTrap two-hybrid system was purchased from Stratagene (La Jolla, CA). The cDNA encoding the full-length open reading frame of human p73α was amplified by PCR using pcDNA3-p73α as template. The PCR product, which was produced by additional upstream 5′-BamHI and downstream 3′-SalI restriction sites, was digested completely with BamHI and SalI; purified on agarose gel; and directly inserted in-frame into the identical restriction sites of pSos to give pSos-p73α. The resulting pSos-p73α"bait" plasmid was used to identify the cDNA encoding the p73α-binding protein from a human fetal brain cDNA library cloned into the pMyr plasmid (Stratagene). The screening was carried out according to the manufacturer's instructions. Briefly, a temperature-sensitive yeast strain (cdc25Hα) was cotransformed with pSos-p73α and the cDNA library using the lithium acetate/heat shock procedure as described previously (29). Transformants were allowed to grow on selection medium containing glucose for 2 days at 25 °C and then transferred onto selection medium containing galactose. Plasmid DNAs were isolated from the colonies exhibiting galactose-dependent growth at 37 °C and transformed into *Escherichia coli*. Finally, the nucleotide sequences of the positive cDNA clones were determined by the dideoxy terminator cycle sequencing using an ABI automated DNA sequencer (Applied Biosystems, Foster City, CA).

Western Blot Analysis—Transfected cells were washed twice with phosphate-buffered saline (PBS) and lysed in ice-cold lysis buffer A (25 mM Tris-Cl (pH 7.5), 137 mM NaCl, 2.7 mM KCl, and 1% Triton X-100) containing protease inhibitor mixture (Sigma). After a brief sonication, whole cell lysates were centrifuged at 15,000 rpm for 10 min at 4 °C to remove insoluble materials, and the protein concentrations of the supernatants were determined using the Bio-Rad protein assay reagent. Protein samples were boiled in SDS sample buffer for 5 min, resolved by 10% SDS-PAGE, and transferred onto Immobilon-P membranes (Millipore, Bedford, MA). The membranes were blocked overnight with 50 mM Tris-Cl (pH 7.6), 100 mM NaCl, and 0.1% Tween 20 containing 5% nonfat dry milk and then incubated at room temperature for 1 h with anti-FLAG monoclonal antibody (M2, Sigma), anti-green fluorescence protein (GFP) monoclonal antibody (1E4, Medical and Biological Laboratories, Nagoya, Japan), anti-p53 monoclonal antibody (DO-1, Oncogene Research Products, Cambridge, MA), anti-p73 monoclonal antibody (Ab-4, NeoMarkers, Inc., Fremont, CA), anti-$p21^{WAF1}$ monoclonal antibody (Ab-1, Oncogene Research Products), anti-PKA-Cα polyclonal antibody (C-20, Santa Cruz Biotechnology, Inc., Santa Cruz, CA), or anti-PKA-Cβ polyclonal antibody (C-20, Santa Cruz Biotechnology, Inc.), followed by incubation with the corresponding horseradish peroxidase-conjugated secondary antibodies (Jackson ImmunoResearch Laboratories, Inc., West Grove, PA). Following the last wash, horseradish peroxidase-labeled antibodies were detected using an enhanced chemiluminescence detection system (ECL, Amersham Biosciences) according to the manufacturer's instructions.

Immunoprecipitation and Pull-down Assay—For immunoprecipitation, cell lysates were prepared in lysis buffer A. Equal amounts of protein extracts were pre-absorbed with protein G-Sepharose beads (Amersham Biosciences) for 1 h at 4 °C, and the precleared lysates were incubated with the indicated antibodies for 2 h at 4 °C, followed by incubation with protein G-Sepharose beads for an additional 1 h at 4 °C. The immune complexes were then washed three times with lysis buffer A, eluted by boiling in SDS sample buffer for 5 min, and subjected to Western blot analysis. For glutathione *S*-transferase (GST) pull-down assays, GST alone or the indicated GST-p73α fusion proteins were expressed in *E. coli* strain DH5α and loaded onto glutathione-Sepharose 4B beads (Amersham Biosciences). PKA-Cβ was generated *in vitro* in the presence of [^{35}S]methionine using the TNT quick-coupled *in vitro* transcription/translation system (Promega Corp., Madison, WI) according to the manufacturer's instructions. ^{35}S-Labeled PKA-Cβ was incubated with GST or GST-p73α fusion proteins bound to glutathione-Sepharose beads for 2 h at 4 °C in a total volume of 400 μl of binding buffer (50 mM Tris-Cl (pH 7.5), 150 mM NaCl, and 0.1% Nonidet P-40). Beads were washed extensively with the same buffer, and the radiolabeled proteins were eluted by boiling in SDS sample buffer for 5 min. Following electrophoresis, gels were destained, dried, and exposed to an x-ray film with an intensifying screen at −80 °C.

Cell Fractionation—Transfected COS-7 cells were fractionated into nuclear and cytoplasmic fractions as described previously (30). In brief, cells were washed twice with ice-cold 1× PBS and lysed in lysis buffer B containing 10 mM Tris-Cl (pH 7.5), 1 mM EDTA, 0.5% Nonidet P-40, and protease inhibitor mixture for 30 min at 4 °C. Cell lysates were centrifuged at 15,000 rpm for 10 min at 4 °C to separate soluble (cytoplasmic) from insoluble (nuclear) fractions. The pellets were washed extensively with lysis buffer B and further dissolved in 1× SDS sample buffer. The nuclear and cytoplasmic fractions were analyzed by immunoblotting with anti-lamin B monoclonal antibody (Ab-1, Oncogene Research Products) or with anti-α-tubulin monoclonal antibody (Ab-2, NeoMarkers, Inc.).

Immunofluorescence Microscopy—H1299 cells were grown on coverslips and transiently cotransfected with the expression plasmids for hemagglutinin (HA)-p73α and FLAG-PKA-Cβ. Forty-eight hours after transfection, cells were fixed with 3.7% formaldehyde in PBS for 30 min at room temperature and permeabilized with 0.2% Triton X-100 for 5 min. Nonspecific binding sites were blocked by treating cells with PBS containing 3% bovine serum albumin. The cells were incubated with anti-HA polyclonal and anti-FLAG monoclonal antibodies for 1 h, followed by incubation with fluorescein isothiocyanate- and rhodamine-conjugated secondary antibodies (Invitrogen). The coverslips were washed with PBS, mounted onto slides, and observed under a Fluoview laser scanning confocal microscope (Olympus, Tokyo, Japan).

Luciferase Reporter Assay—p53-deficient H1299 cells (5×10^4 cells in a 12-well plate) were transiently cotransfected with a constant amount of the indicated expression plasmid (HA-p73α, HA-p73β, or p53), a p53/p73-responsive luciferase reporter construct ($p21^{WAF1}$ or *bax*), and pRL-TK encoding *Renilla* luciferase with or without increasing amounts of the expression plasmid for FLAG-PKA-Cβ. The total amount of DNA was kept constant (510 ng) with pcDNA3 per transfection. Forty-eight hours after transfection, cells were lysed and assayed for luciferase activity using the Dual-Luciferase reporter assay system (Promega Corp.) according to the manufacturer's recommendations. The transfection efficiency was normalized based on pRL-TK reporter activity.

Reverse Transcription-PCR—H1299 cells were transiently cotransfected with the indicated combinations of expression plasmids. Twenty-four hours after transfection, total RNA was prepared using an RNeasy mini kit (Qiagen Inc.) according to the manufacturer's protocol. One microgram of total RNA was used to synthesize the first-strand cDNA using random primers and SuperScript II reverse transcriptase (Invitrogen). Reverse transcription was carried out at 42 °C for 90 min, and reverse transcripts were amplified by standard PCR with *rTaq* DNA polymerase (Takara, Ohtsu, Japan). The primers used for PCR were as follows: $p21^{WAF1}$, 5′-ATGAAATTCACCCCCTTTCC-3′ (sense) and 5′-CCCTAGGCTGTGCTCACTTC-3′ (antisense); and glyceraldehyde-3-phosphate dehydrogenase, 5′-ACCTGACCTGCCGTCTAGAA-3′

[1] The abbreviations used are: PKA-C, protein kinase A catalytic subunit; PBS, phosphate-buffered saline; GFP, green fluorescence protein; GST, glutathione *S*-transferase; HA, hemagglutinin; ChIP, chromatin immunoprecipitation; Bt_2cAMP, dibutyryl cAMP.

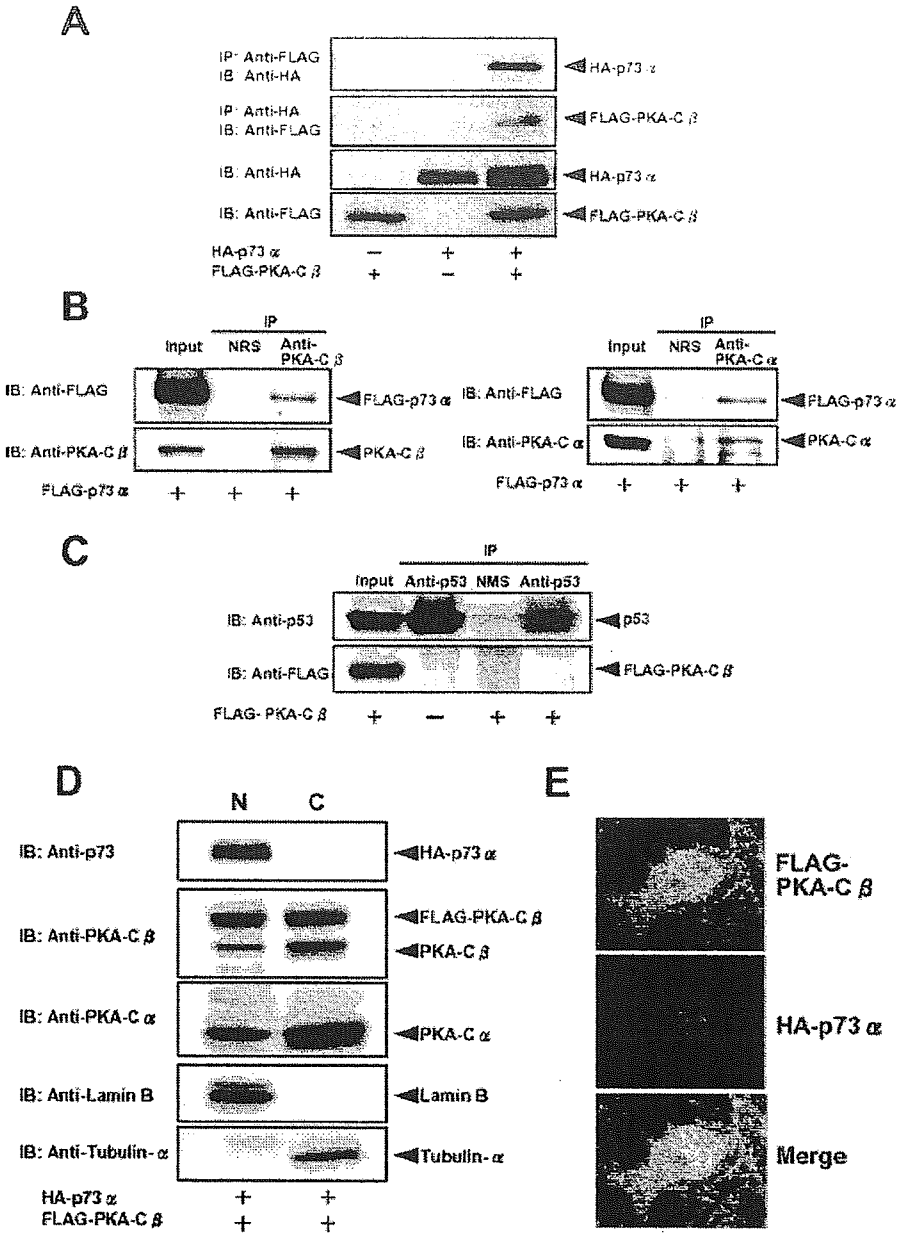

FIG. 1. **Interaction between p73 and PKA-Cβ in mammalian cultured cells.** *A*, p73α forms a complex with PKA-Cβ in COS-7 cells. Whole cell lysates prepared from COS-7 cells transiently cotransfected with the indicated combinations of expression plasmids were immunoprecipitated (*IP*) with anti-FLAG or anti-HA monoclonal antibody. Immunoprecipitates were analyzed by immunoblotting (*IB*) with anti-HA (*first panel*) or anti-FLAG (*second panel*) monoclonal antibody. Whole cell lysates were immunoblotted with anti-HA (*third panel*) or anti-FLAG (*fourth panel*) monoclonal antibody to show the expression of HA-p73α or FLAG-PKA-Cβ, respectively. *B*, p73α binds to endogenous PKA-C in COS-7 cells. COS-7 cells were transiently transfected with the expression plasmid for FLAG-p73α. Forty-eight hours after transfection, whole cell lysates were prepared and subjected to immunoprecipitation with anti-PKA-Cβ (*left panels*) or anti-PKA-Cα (*right panels*) polyclonal antibody. Immunoprecipitation with normal rabbit serum (*NRS*) was used as a negative control. After immunoprecipitation, coprecipitating FLAG-p73α was detected by immunoblotting with anti-FLAG monoclonal antibody. *C*, PKA-Cβ does not bind to endogenous p53. COS-7 cells were transiently transfected with the empty control plasmid or with the expression plasmid encoding FLAG-PKA-Cβ. Forty-eight hours post-transfection, whole cell lysates were prepared and subjected to immunoprecipitation with anti-p53 monoclonal antibody or normal mouse serum (*NMS*), followed by immunoblotting with anti-p53 (*upper panel*) or anti-FLAG (*lower panel*) monoclonal antibody. *D*, subcellular localization of exogenous and endogenous PKA-Cβ. p53-deficient H1299 cells were transiently cotransfected with the expression plasmids for HA-p73α and FLAG-PKA-Cβ (*first* through *third panels*). Forty-eight hours after transfection, transfected cells were fractionated into nuclear (*N*) and cytoplasmic (*C*) fractions as described under "Experimental Procedures." Each fraction was adjusted to an equal volume, and the aliquots of these fractions were separated by 10% SDS-PAGE, followed by immunoblotting with the indicated antibodies. These fractions were analyzed for lamin B (*fourth panel*) and α-tubulin (*fifth panel*) to show the validity of our fractionation technique. *E*, nuclear co-localization of p73 and PKA-Cβ. H1299 cells plated on coverslips were cotransfected with the expression plasmids for HA-p73α and FLAG-PKA-Cβ and processed for immunocytochemical detection using anti-HA and anti-FLAG antibodies. The merged image shows the nuclear co-localization of p73α and PKA-Cβ.

(sense) and 5′-TCCACCACCCTGTTGCTGTA-3′ (antisense). PCR products were separated by 1.5% agarose gel electrophoresis and stained with ethidium bromide.

In Vitro Kinase Assays—GST or the indicated GST-p73α fusion proteins bound to glutathione-Sepharose beads were washed three times with kinase buffer (20 mM Tris-Cl (pH 7.5), 100 mM NaCl, and 12 mM $MgCl_2$). The washed beads were incubated with 30 μl of kinase buffer containing 2 units of purified PKA catalytic subunit (Sigma), 2 mM

dithiothreitol, and 10 μCi of [γ-^{32}P]ATP for 30 min at 4 °C. The reaction mixtures were boiled in 2× SDS sample buffer for 5 min, and the proteins were separated by 10% SDS-PAGE. The gels were dried and processed for autoradiography.

Cell Survival Assays—H1299 cells were seeded in 6-well plates and allowed to attach. Cells were then cotransfected with the indicated expression plasmids. Twenty-four hours after transfection, cells were exposed to camptothecin (final concentration of 1 μM) for 24 h. Cell viability was measured by a colorimetric assay with modified 3-(4,5-dimethylthiazol-2-yl)-2,5-diphenyltetrazolium bromide as the substrate.

Construction of a Kinase-deficient Mutant of PKA-Cβ—The K76R mutation was introduced into wild-type PKA-Cβ by PCR-based mutagenesis using *PfuUltra*™ high fidelity DNA polymerase (Stratagene) according to the manufacturer's protocol. The following oligonucleotide primers were used: 5′-AGGATCTTAGATAAGCAGAAGGTT-3′ (the underlined segment encodes Arg at position 76) and 5′-CATGGCATAATACTGTTCAGTGGCT-3′. This yielded the expression plasmid pcDNA3-FLAG-PKA-Cβ(K76R), which was completely sequenced by the dideoxy chain termination method.

Chromatin Immunoprecipitation (ChIP)—ChIP assays were performed following a protocol provided by Upstate Biotechnology, Inc. (Lake Placid, NY). In brief, H1299 cells were transiently cotransfected with the expression plasmids for HA-p73α (1.2 μg) and FLAG-PKA-Cβ (4.8 μg). Thirty-six hours after transfection, cells were cross-linked with 1% formaldehyde in medium for 15 min at 37 °C. Cells were then washed with ice-cold PBS and resuspended in 200 μl of SDS-sample buffer containing protease inhibitor mixture. The suspension was sonicated 10 times for 30 s with a 1-min cooling period on ice between times and precleared with 20 μl of protein A-agarose beads blocked with sonicated salmon sperm DNA for 30 min at 4 °C. The beads were removed, and the chromatin solution was immunoprecipitated overnight with anti-HA monoclonal antibody at 4 °C, followed by incubation with protein A-agarose beads for an additional 1 h at 4 °C. The immune complexes were eluted with 100 μl of elution buffer (1% SDS and 0.1 M $NaHCO_3$) and formaldehyde cross-links were reversed by heating at 65 °C for 6 h. Proteinase K was added to the reaction mixtures and incubated at 45 °C for 1 h. DNAs of the immunoprecipitates and control input DNAs were purified using a QIAquick PCR purification kit (Qiagen Inc.) and then analyzed by regular PCR using the human p21^{WAF1} and *bax* promoter-specific primers. The primer sequences were 5′-CACCTTTCACCATTCCCCTA-3′ and 5′-GCAGCCCAAGGACAAAATAG-3′ for p21^{WAF1} and 5′-AAAGCTCAGAGGCCCAAAAT-3′ and 5′-AGGCTGAGACGGGGTTATCT-3′ for *bax*.

RESULTS

Identification of PKA-Cβ as a Novel Binding Partner of p73—Because the conventional yeast two-hybrid system depends on the DNA binding as well as the transactivation function of Gal4, it is quite difficult to use a full-length transcriptional regulator with a transactivation domain as bait. To identify potential p73-interacting cellular protein(s), we used full-length p73α as bait in a new CytoTrap yeast two-hybrid screen relying on the Sos recruitment system. A temperature-sensitive yeast strain (cdc25Hα) was cotransformed with a bait plasmid and a human fetal brain cDNA library. Of a total of 1 × 10^6 primary transformants grown on medium containing glucose at 30 °C, one clone (termed F115) exhibited galactose-dependent growth at 37 °C. The plasmid DNA derived from the cDNA library was introduced into *E. coli*, and its nucleotide sequence was determined. Sequence analysis revealed that the F115 cDNA clone encodes full-length PKA-Cβ. Of the PKA catalytic subunit isoforms (PKA-Cα, PKA-Cβ, and PKA-Cγ), PKA-Cβ is highly expressed in brain and reproductive tissues, whereas PKA-Cα is ubiquitously expressed in mammalian tissues (31, 32).

PKA-Cβ Associates with p73 in Mammalian Cultured Cells—To confirm the interaction between PKA-Cβ and p73 detected by the CytoTrap yeast two-hybrid system, co-immunoprecipitation experiments were carried out using whole cell lysates prepared from COS-7 cells expressing exogenous FLAG-PKA-Cβ and HA-p73α. As shown in Fig. 1A, the anti-FLAG immunoprecipitates contained HA-p73α. Used as a control, HA-p73α was not detectable in the anti-FLAG immunoprecipitates of COS-7 cells expressing FLAG-PKA-Cβ or HA-p73α alone. Analysis of the anti-HA immunoprecipitates also demonstrated that FLAG-PKA-Cβ co-immunoprecipitated with HA-p73α. Next, we examined whether endogenous PKA-Cβ could interact with p73α. To this end, whole cell lysates prepared from COS-7 cells transfected with the expression plasmid for FLAG-p73α were immunoprecipitated with normal rabbit serum or with the specific antibody against PKA-Cβ, followed by immunoblotting with anti-FLAG anti-

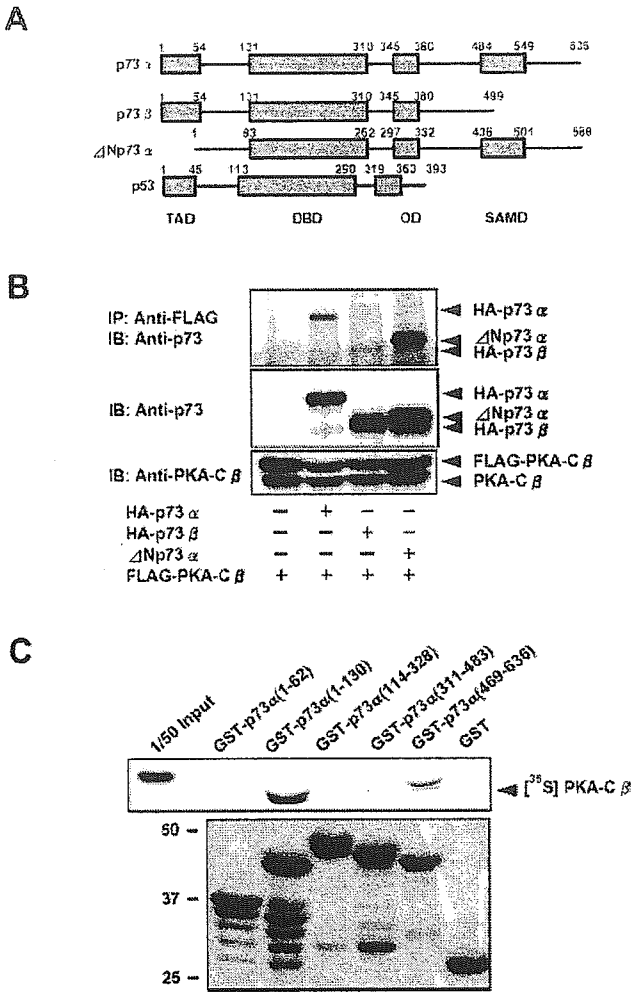

FIG. 2. **Interacting region within p73 for PKA-Cβ.** *A*, domain structures of p73 and p53. The transactivation domain (*TAD*), DNA-binding domain (*DBD*), oligomerization domain (*OD*), and sterile α motif domain (*SAMD*) are indicated. The *numbers* above the p73 variants and p53 indicate amino acid numbering. *B*, interaction of PKA-Cβ with various p73 variants. Whole cell lysates prepared from H1299 cells transiently cotransfected with the expression plasmid for HA-p73α, HA-p73β, or ΔNp73α and with the expression plasmid for FLAG-PKA-Cβ were immunoprecipitated (*IP*) with anti-FLAG monoclonal antibody. The immune complexes were analyzed by immunoblotting (*IB*) with anti-p73 monoclonal antibody (*upper panel*). The expression levels of p73 variants (*middle panel*) and PKA-Cβ (*lower panel*) in whole cell lysates were monitored by immunoblotting with the indicated antibodies. *C*, *in vitro* GST pull-down assays. Bacterially expressed GST or the indicated GST-p73α fusion proteins were incubated with *in vitro* translated ^{35}S-labeled FLAG-PKA-Cβ and precipitated with glutathione-Sepharose 4B beads (50% slurry). After extensive washing, the bound proteins were separated by 10% SDS-PAGE and processed for autoradiography (*upper panel*). *1/50 Input* indicates the radiolabeled FLAG-PKA-Cβ used for *in vitro* pull-down assays that was directly loaded on the same gel as a control. GST and GST-p73α fusion proteins were stained with Coomassie Brilliant Blue (*lower panel*). The positions of molecular mass markers are indicated on the left in kilodaltons.

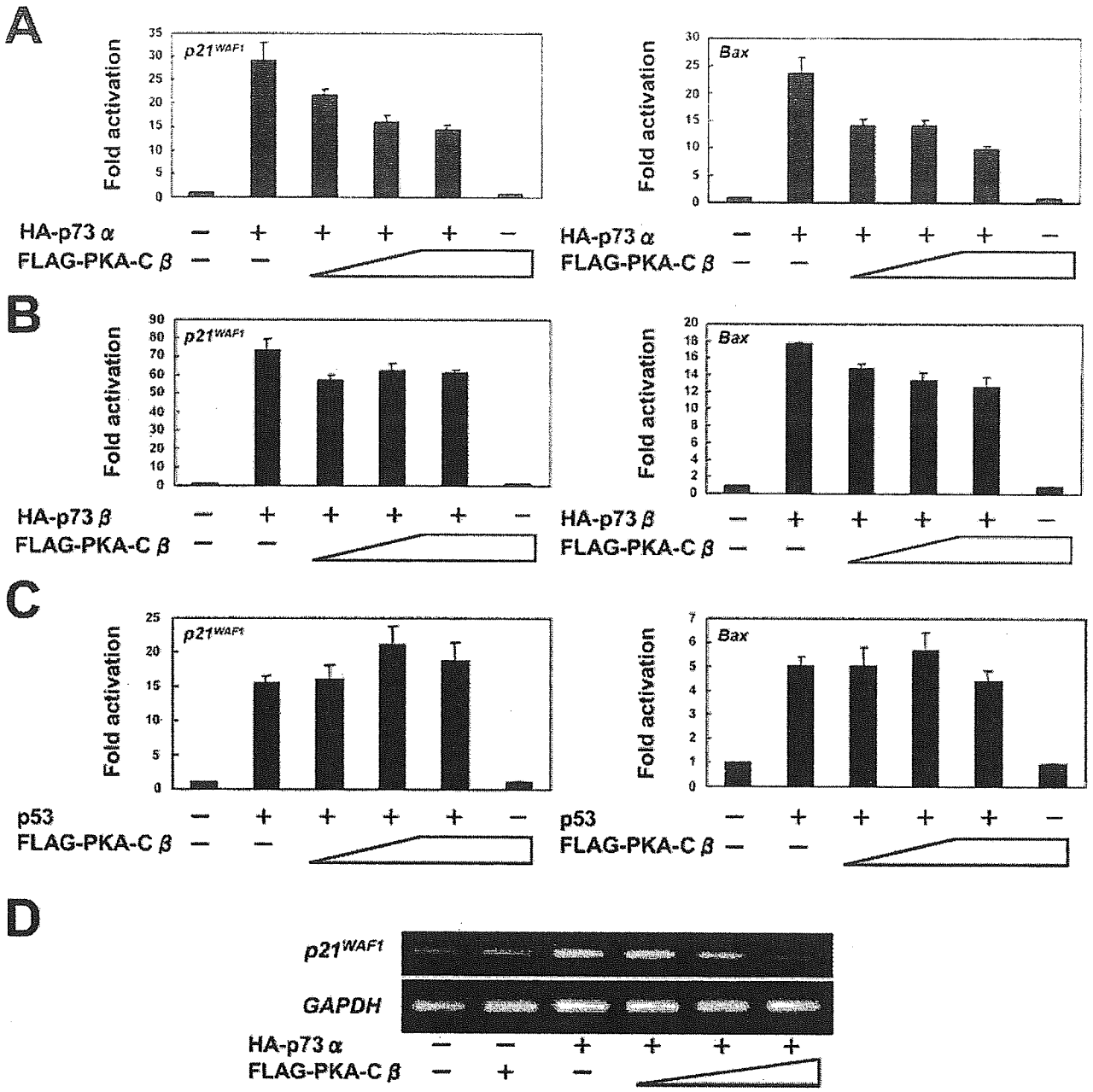

FIG. 3. **PKA-Cβ inhibits p73α-mediated transcriptional activation.** *A–C*, luciferase reporter assays. H1299 cells (5×10^4 cells/12-well plates) were transiently cotransfected with 25 ng of the expression plasmid for HA-p73α (*A*), HA-p73β (*B*), or p53 (*C*); 100 ng of the luciferase reporter construct containing the p53/p73-responsive element derived from the $p21^{WAF1}$ (*left panels*) or *bax* (*right panels*) promoter; and 10 ng of *Renilla* luciferase plasmid (pRL-TK) with or without increasing amounts of the expression plasmid for FLAG-PKA-Cβ (25, 50, and 100 ng). The total amount of the plasmid DNA per transfection was kept constant (510 ng) with pcDNA3. All transfections were performed in triplicate. Luciferase activity was measured 48 h post-transfection. The transfection efficiency was standardized for *Renilla* luciferase activity. The -fold increase in luciferase activity is compared with that in cells transfected with pcDNA3 alone. *D*, reverse transcription-PCR analysis. Total RNA prepared from H1299 cells transiently cotransfected with a constant amount of the expression plasmid for HA-p73α (200 ng) with or without increasing amounts of the expression plasmid for FLAG-PKA-Cβ (200, 400, and 800 ng) was subjected to reverse transcription-PCR analysis for endogenous $p21^{WAF1}$ mRNA expression (*upper panel*). Glyceraldehyde-3-phosphate dehydrogenase (*GAPDH*) mRNA expression levels were used as an internal control (*lower panel*).

body. As shown in Fig. 1*B* (*upper panels*), FLAG-p73α co-immunoprecipitated with endogenous PKA-Cβ. Because the amino acid sequences of PKA-Cα and PKA-Cβ are 91% identical (31), we examined whether endogenous PKA-Cα could bind to p73α. Co-immunoprecipitation experiments revealed that, like PKA-Cβ, endogenous PKA-Cα associated with FLAG-p73α (Fig. 1*B*, *lower panels*). In sharp contrast to p73α, p53 failed to interact with FLAG-PKA-Cβ under our experimental conditions (Fig. 1*C*).

To investigate the subcellular distribution of PKA-Cβ in the presence of exogenous p73α, we employed the biochemical fractionation of transfected H1299 cells. H1299 cells transiently cotransfected with the expression plasmids for HA-p73α and FLAG-PKA-Cβ were fractionated into nuclear and cytoplasmic fractions, and the fractions obtained were subjected to immunoblotting with the indicated antibodies. The purity of the nuclear and cytoplasmic fractions was verified by immunoblotting with anti-lamin B and anti-α-tubulin antibodies, respec-

tively. As shown in Fig. 1*D*, HA-p73α was detected exclusively in the nuclear fractions, whereas FLAG-PKA-Cβ and endogenous PKA-Cβ and PKA-Cα were present in both the cytoplasmic and nuclear fractions. As expected, confocal microscopy of immunostained H1299 cells expressing FLAG-PKA-Cβ and HA-p73α revealed that both proteins co-localized in the cell nucleus (Fig. 1*E*).

Identification of the Interacting Region within p73—To examine which region(s) of p73 could be engaged in the interaction with PKA-Cβ, we performed co-immunoprecipitation and GST pull-down experiments. Fig. 2*A* depicts the domain structures of various p73 variants used for co-immunoprecipitation experiments. Whole cell lysates prepared from H1299 cells transiently cotransfected with the indicated combinations of expression plasmids were immunoprecipitated with anti-FLAG antibody, followed by immunoblotting with anti-p73 antibody. As shown in Fig. 2*B*, HA-p73α and ΔNp73α co-purified with FLAG-PKA-Cβ, whereas the binding of HA-p73β to FLAG-PKA-Cβ was significantly weaker than seen with HA-p73α and ΔNp73α, suggesting that the C-terminal region of p73α might be required for the interaction with PKA-Cβ. To verify these results, *in vitro* GST pull-down assays were carried out using a series of GST-p73α fusion proteins. *In vitro* translated ^{35}S-labeled FLAG-PKA-Cβ was incubated with glutathione-Sepharose beads complexed either with GST alone or with GST-p73α. The autoradiogram in Fig. 2*C* (*upper panel*) shows that GST-p73α-(1–130) and GST-p73α-(469–636) were able to interact with FLAG-PKA-Cβ. The Coomassie Brilliant Blue staining shown in Fig. 2*C* (*lower panel*) revealed that the glutathione-Sepharose beads contained equal amounts of GST-p73α fusion proteins. Taken together, our results suggest that both the N-terminal (amino acids 63–130) and C-terminal (amino acids 469–636) regions of p73α might be essential for the interaction with PKA-Cβ.

PKA-Cβ Inhibits p73α-mediated Transcriptional Activation—In view of the ability of PKA-Cβ to interact with p73α, we next examined whether PKA-Cβ could affect p73α function as a transcriptional regulator. For this purpose, p53-deficient H1299 cells were transiently cotransfected with a constant amount of the expression plasmid for HA-p73α, HA-p73β, or p53 together with the luciferase reporter construct controlled by the p53/p73-responsive element from the p21^{WAF1} or *bax* promoter in the presence or absence of increasing amounts of the expression plasmid for FLAG-PKA-Cβ. All cotransfections included pRL-TK to monitor transfection efficiency, and controls included cotransfections with the empty control plasmid. As shown in Fig. 3*A*, coexpression of FLAG-PKA-Cβ and HA-p73α resulted in marked repression of the p21^{WAF1}- and *bax*-luciferase activities induced by HA-p73α in a dose-dependent manner, and FLAG-PKA-Cβ alone had no effect on the reporter gene activity. In contrast, FLAG-PKA-Cβ had no obvious effects on p73β- and p53-mediated transcriptional activation (Fig. 3, *B* and *C*). These results strongly suggest that there is a correlation between the capacity of PKA-Cβ to interact with p73 or p53 and its ability to inhibit their transactivation function. To determine whether PKA-Cβ could inhibit the p73α-mediated transcriptional activation of endogenous p21^{WAF1}, we performed reverse transcription-PCR analysis using total RNA prepared from H1299 cells transiently cotransfected with the indicated combinations of expression plasmids. As shown in Fig. 3*D*, ectopic expression of HA-p73α resulted in a remarkable up-regulation of endogenous p21^{WAF1} expression, and coexpression of FLAG-PKA-Cβ and HA-p73α inhibited the p73α-mediated induction of p21^{WAF1} in a dose-dependent manner.

To further confirm the inhibitory effect of PKA-Cβ on the transcriptional activity of p73α, H1299 cells were transiently

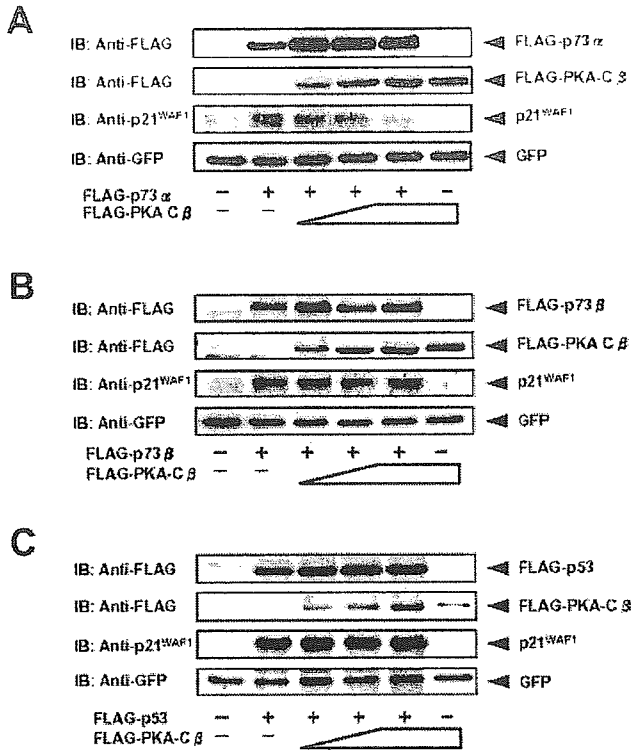

FIG. 4. **PKA-Cβ inhibits the p73α-dependent accumulation of endogenous p21^{WAF1}.** H1299 cells were transiently cotransfected with 200 ng of the expression plasmid for FLAG-p73α (*A*), FLAG-p73β (*B*), or FLAG-p53 (*C*) and 50 ng of the GFP expression plasmid with or without increasing amounts of the expression plasmid for FLAG-PKA-Cβ (200, 400, and 800 ng). Thirty-six hours after transfection, whole cell lysates were prepared and subjected to immunoblotting (*IB*) with the indicated antibodies (*first* through *third panels*). The GFP expression plasmid was included in each transfection as a transfection efficiency control, and the expression levels of GFP were detected with anti-GFP monoclonal antibody (*fourth panels*).

cotransfected with a constant amount of the expression plasmid for FLAG-p73α, FLAG-p73β, or FLAG-p53 with or without increasing amounts of the expression plasmid for FLAG-PKA-Cβ, and the protein levels of endogenous p21^{WAF1} were determined by immunoblotting. As shown in Fig. 4*A*, endogenous p21^{WAF1} was increased by ectopic FLAG-p73α expression, whereas overexpression of FLAG-PKA-Cβ resulted in a reduction in the level of endogenous p21^{WAF1} induced by FLAG-p73α, supporting the notion that PKA-Cβ inhibits the transcriptional activity of p73α. In contrast, PKA-Cβ had no detectable effects on the p73β- or p53-dependent induction of endogenous p21^{WAF1} (Fig. 4, *B* and *C*), consistent with the results obtained by luciferase reporter analysis. In addition, coexpression of FLAG-p73α and FLAG-PKA-Cβ resulted in a slight increase in the amounts of FLAG-p73α, whereas FLAG-PKA-Cβ had a negligible effect on the amounts of FLAG-p73β and FLAG-p53 (Fig. 4). FLAG-p73α decayed at slower rates in the presence of FLAG-PKA-Cβ than in its absence (data not shown); however, its physiological implications remain to be determined.

PKA-Cβ Phosphorylates p73—To determine whether p73 could be a substrate for PKA-Cβ, the GST-p73α fusion proteins used for the *in vitro* pull-down assay were incubated with the commercially available PKA catalytic subunit purified from bovine heart and [γ-^{32}P]ATP. Of the GST-p73α fusion proteins tested, only GST-p73α-(1–130) was phosphorylated by the PKA catalytic subunit (Fig. 5*A*). The N-terminal region of p73α might be involved in phosphorylation by the PKA catalytic subunit.

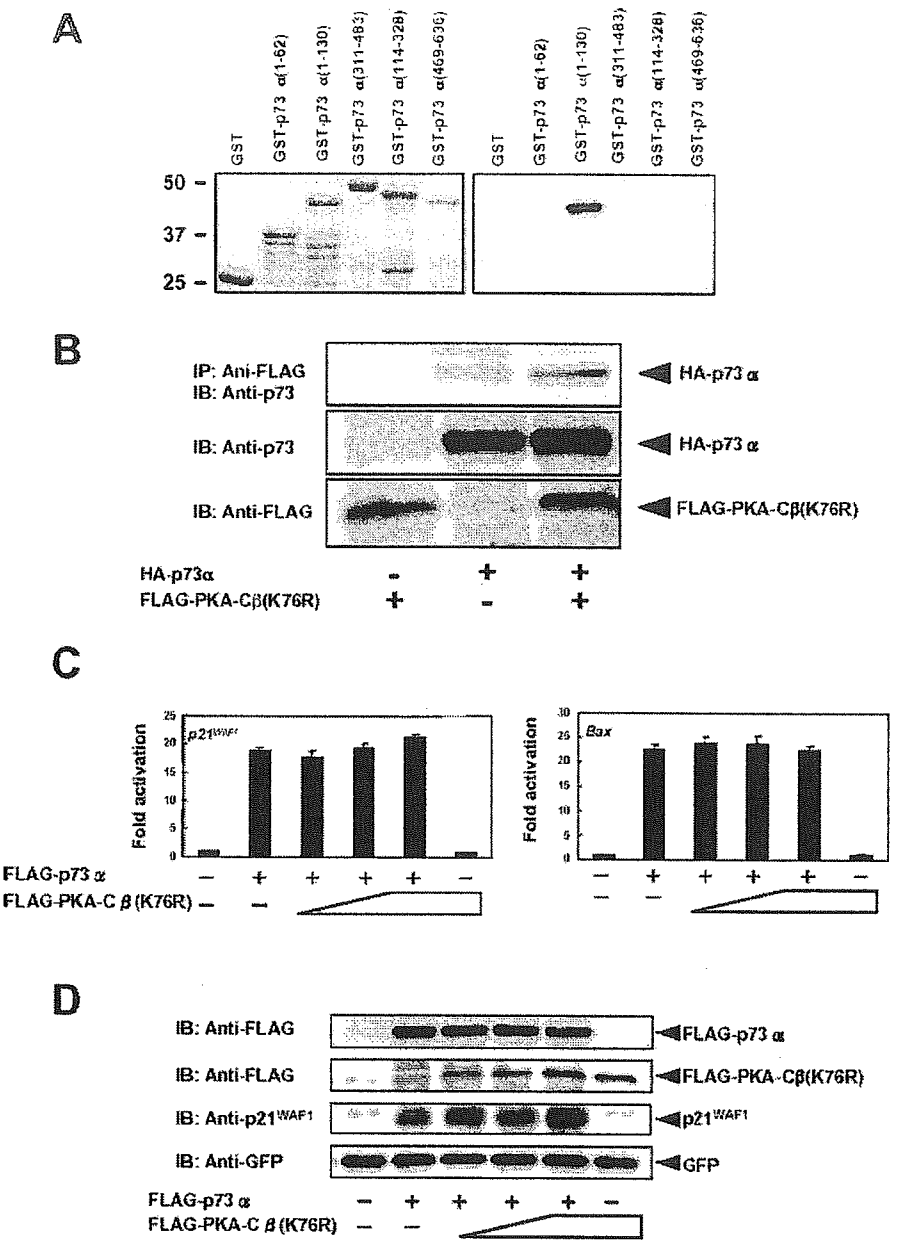

FIG. 5. **PKA-Cβ phosphorylates p73α, and the kinase-deficient mutant of PKA-Cβ fails to inhibit the transcriptional activity of p73α.** *A*, PKA-Cβ can phosphorylate p73α *in vitro*. GST or GST-p73α fusion proteins bound to glutathione-Sepharose beads were incubated with the purified catalytic subunit of PKA in the presence of [γ-^{32}P]ATP for 30 min at 30 °C. Samples were then directly boiled in 2× SDS sample buffer prior to loading them onto 10% SDS-polyacrylamide gels. Following electrophoresis, gels were dried and processed for autoradiography (*right panel*). GST and GST-p73α fusion proteins were stained with Coomassie Brilliant Blue and used for *in vitro* kinase assay (*left panel*). The positions of molecular mass markers are shown on the left in kilodaltons. *B*, kinase-deficient PKA-Cβ retains the ability to interact with p73α. Whole cell lysates prepared from COS-7 cells transiently cotransfected with the indicated combinations of expression plasmids were immunoprecipitated (*IP*) with anti-FLAG monoclonal antibody, and the immunoprecipitates were analyzed by immunoblotting (*IB*) with anti-p73 monoclonal antibody (*upper panel*). Lysates not subjected to immunoprecipitation were analyzed by immunoblotting with anti-p73 (*middle panel*) or anti-FLAG (*lower panel*) monoclonal antibody. *C*, luciferase reporter analysis. H1299 cells were transiently cotransfected with a constant amount of the expression plasmid encoding FLAG-p73α, the luciferase reporter construct carrying the p53/p73-responsive element derived from the p21^{WAF1} (*left panel*) or *bax* (*right panel*) promoter, and pRL-TK in the presence or absence of increasing amounts of the expression plasmid for FLAG-PKA-Cβ(K76R). Forty-eight hours after transfection, luciferase activity was determined as described in the legend to Fig. 4. *D*, PKA-Cβ(K76R) has no detectable effect on the p73α-dependent induction of endogenous p21^{WAF1}. H1299 cells were transiently cotransfected with 200 ng of the expression plasmid for FLAG-p73α and 50 ng of the GFP expression plasmid with or without increasing amounts of the expression plasmid for FLAG-PKA-Cβ(K76R) (200, 400, and 800 ng). Thirty-six hours after transfection, whole cell lysates were prepared and analyzed by immunoblotting for the expression levels of endogenous p21^{WAF1}. The GFP expression plasmid was included as a control for transfection efficiency.

Next, we examined whether the inhibitory effect of PKA-Cβ on the transcriptional activity of p73α is dependent on its kinase activity. As described previously (33, 34), PKA-Cβ(K76R), in which Lys-76 within the ATP-binding motif is replaced with Arg, showed very little catalytic activity. We therefore constructed an expression plasmid for FLAG-PKA-Cβ(K76R) and tested whether PKA-Cβ(K76R) could bind to p73α and also repress p73α-mediated transcriptional activation. Co-immunoprecipitation experiments demonstrated that, like wild-type PKA-Cβ, the kinase-deficient form of PKA-Cβ bound to FLAG-p73α in cells (Fig. 5*B*). Notably, luciferase reporter analysis revealed that FLAG-PKA-Cβ(K76R) had little effect on the ability of p73α to drive transcription from the p21^{WAF1} and *bax* promoters (Fig. 5*C*). In accordance with the results from luciferase reporter analysis, FLAG-PKA-Cβ(K76R) failed to reduce the expression levels of endogenous p21^{WAF1} induced by FLAG-p73α as examined by immunoblotting (Fig. 5*D*). Taken together, these results strongly suggest that PKA-Cβ inhibits p73α-mediated transcriptional activation by a kinase activity-dependent mechanism.

Reduction in the Pro-apoptotic Activity of p73α by PKA-Cβ upon DNA Damage—To extend the functional consequences of the interaction between p73α and PKA-Cβ, we investigated whether PKA-Cβ could affect the pro-apoptotic function of p73α in response to DNA damage. For this purpose, we used a low apoptotic dose of camptothecin to facilitate the detection of a potential induction mediated by p73α. H1299 cells were transiently cotransfected with the expression plasmid for FLAG-p73α or FLAG-p53 with or without the expression plasmid encoding FLAG-PKA-Cβ or FLAG-PKA-Cβ(K76R) and then treated with camptothecin at a final concentration of 1 μM for 24 h. After camptothecin action, cell viability was examined by cell survival assay. As shown in Fig. 6*A*, H1299 cells expressing FLAG-p73α alone exhibited an enhanced sensitivity to apoptosis following exposure to camptothecin, which was consistent with previous observations (35). Of note, coexpression of FLAG-PKA-Cβ and FLAG-p73α resulted in a reduction in the cellular

sensitivity to camptothecin, whereas kinase-deficient PKA-Cβ had no significant effect on cell viability. As was also observed in H1299 cells expressing FLAG-p73α, ectopic expression of FLAG-p53 enhanced camptothecin-induced apoptosis (Fig. 6*B*). In sharp contrast to p73α, wild-type or kinase-deficient PKA-Cβ had a negligible effect on p53.

cAMP Analog Inhibits p73α-mediated Transcriptional Activation—Given the inhibitory effect of exogenous PKA-Cβ on p73α in transfected cells, we sought to determine whether the activation of PKA attenuates p73α-mediated transcriptional activation. H1299 cells were transiently cotransfected with or without the expression plasmid for HA-p73α along with the luciferase reporter construct driven by the p53/p73-responsive element from the $p21^{WAF1}$ or *bax* promoter. Twenty-four hours after transfection, cells were either left untreated or treated with the PKA-activating agent dibutyryl cAMP (Bt_2cAMP) in the presence or absence of the PKA inhibitor H-89. As shown in Fig. 7*A*, Bt_2cAMP treatment inhibited p73α-induced $p21^{WAF1}$ and *bax* promoter activation. Intriguingly, the inhibitory effect of Bt_2cAMP was attenuated when cells were exposed to H-89. Under the identical experimental conditions, endogenous $p21^{WAF1}$ was significantly induced by exogenously expressed HA-p73α (Fig. 7*B*). Densitometric scanning of the immunoblot revealed that Bt_2cAMP treatment decreased the level of $p21^{WAF1}$ by 29% relative to that induced by HA-p73α, and the $p21^{WAF1}$ level was partially restored in the presence of H-89, in accordance with the results obtained by luciferase reporter analysis. Thus, it is likely that the elevation of intracellular cAMP and the subsequent PKA activation contribute to the reduction in p73α-mediated transcriptional activation.

PKA-Cβ Stimulates the Intramolecular Interaction of p73—To clarify the precise molecular mechanism by which PKA-Cβ impairs the transcriptional activity of p73α, we performed ChIP analysis. Cross-linked chromatin prepared from H1299 cells transiently cotransfected with the indicated combinations of expression plasmids was immunoprecipitated with anti-HA antibody, followed by amplification with the indicated promoter-specific primers. Under our experimental conditions, HA-p73α was efficiently recruited to the $p21^{WAF1}$ and *bax* promoters in the absence of exogenous PKA-Cβ (Fig. 8*A*). No significant decrease in chromatin binding was detected in cells expressing HA-p73α and FLAG-PKA-Cβ, suggesting that PKA-Cβ has little effect on the sequence-specific DNA binding activity of p73α.

It has been reported recently that the extreme C-terminal regions of p73α and p63α (another member of the p53 family) have an inhibitory effect on their transactivation potential (7, 36, 37). To assess whether the C-terminal inhibitory domain of p73α could be involved in the PKA-Cβ-mediated down-regulation of p73α, we performed additional luciferase reporter analyses in H1299 cells cotransfected with the expression plasmid for HA-p73α-(1–548) and FLAG-PKA-Cβ. As shown in Fig. 8*B* (*upper panel*), HA-p73α-(1–548), which lacks the extreme C-terminal extension of wild-type p73α, interacted with FLAG-PKA-Cβ as determined by co-immunoprecipitation experiments. It is worth noting that, in contrast to wild-type p73α, FLAG-PKA-Cβ had no detectable effect on the transcriptional activity of HA-p73α-(1–548) (Fig. 8*B*, *lower panel*), indicating that the extreme C-terminal region of p73α plays a critical role in the PKA-Cβ-mediated inhibition of p73α.

Serber *et al.* (37) reported that the extreme C-terminal domain binds to the N-terminal transactivation domain of p63 and inhibits its transactivation potential. Considering that PKA-Cβ interacts with p73α through its N- and C-terminal domains, it is possible that PKA-Cβ could stimulate the intramolecular interaction between the two domains of p73α, thereby inhibiting its transcriptional activity. To test this possibility, we performed co-immunoprecipitation analysis. Whole cell lysates prepared from COS-7 cells transiently transfected with the indicated combinations of expression plasmids were immunoprecipitated with anti-p73 antibody, followed by immunoblotting with anti-HA antibody, and the possible effect of FLAG-PKA-Cβ on the complex formation between HA-p73α-(1–247) and FLAG-p73α-(247–636) was examined. The anti-p73 antibody used for this assay recognizes the C-terminal portion of p73 and thus does not detect p73α-(1–247). As shown in Fig. 8*C*, HA-p73α-(1–247) efficiently co-immunoprecipitated with FLAG-p73α-(247–636) in the presence of FLAG-PKA-Cβ, whereas FLAG-PKA-Cβ(K76R) had a negligible effect on the complex formation between HA-p73α-(1–247) and FLAG-p73α-(247–636). The few complexes observed in the absence of FLAG-PKA-Cβ could be due to endogenous PKA-Cβ. These results strongly suggest that FLAG-PKA-Cβ contributes to the intramolecular interaction of p73α between the N-terminal transactivation and C-terminal inhibitory domains.

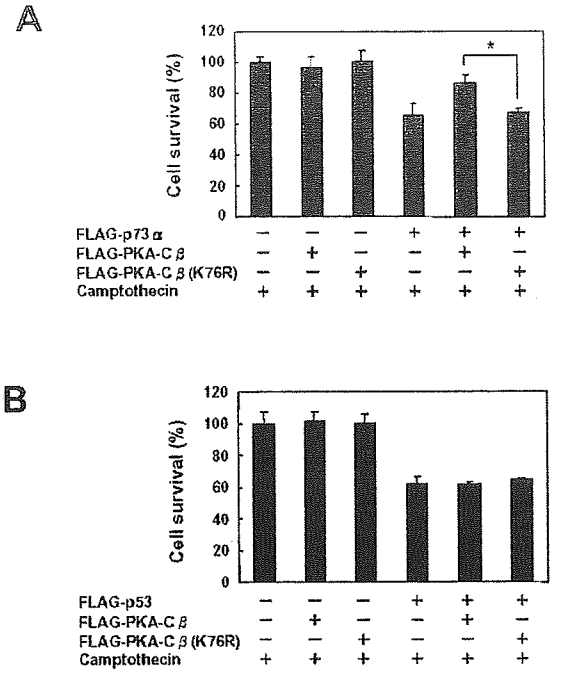

FIG. 6. **p73α-mediated increase in sensitivity to camptothecin is suppressed by wild-type PKA-Cβ, but not by kinase-deficient PKA-Cβ.** H1299 cells were transiently cotransfected with the expression plasmid for FLAG-p73α (*A*) or FLAG-p53 (*B*) with or without the expression plasmid encoding FLAG-PKA-Cβ or FLAG-PKA-Cβ(K76R). Twenty-four hours after transfection, cells were exposed to camptothecin (final concentration of 1 μM) for 24 h, and their viability was evaluated by 3-(4,5-dimethylthiazol-2-yl)-2,5-diphenyltetrazolium bromide assay. *, $p < 0.01$ *versus* +FLAG-PKA-Cβ.

DISCUSSION

In this study, we have screened a human fetal brain cDNA library using a new CytoTrap yeast two-hybrid screening method based on the Sos recruitment system and identified, for the first time, PKA-Cβ as a p73α-binding protein. PKA-Cβ associated with p73α through its N- and C-terminal regions in mammalian cultured cells and significantly inhibited its transactivation function. Under our experimental conditions, PKA-Cβ, which did not bind to p53, had a negligible effect on p53. Intriguingly, PKA-Cβ might bridge the N-terminal transactivation and C-terminal inhibitory domains of p73α, thereby rendering p73α a latent inactive form. *In vitro* kinase assay demonstrated that PKA can phosphorylate p73, and the kinase-deficient mutant of PKA-Cβ (PKA-Cβ(K76R)) failed to

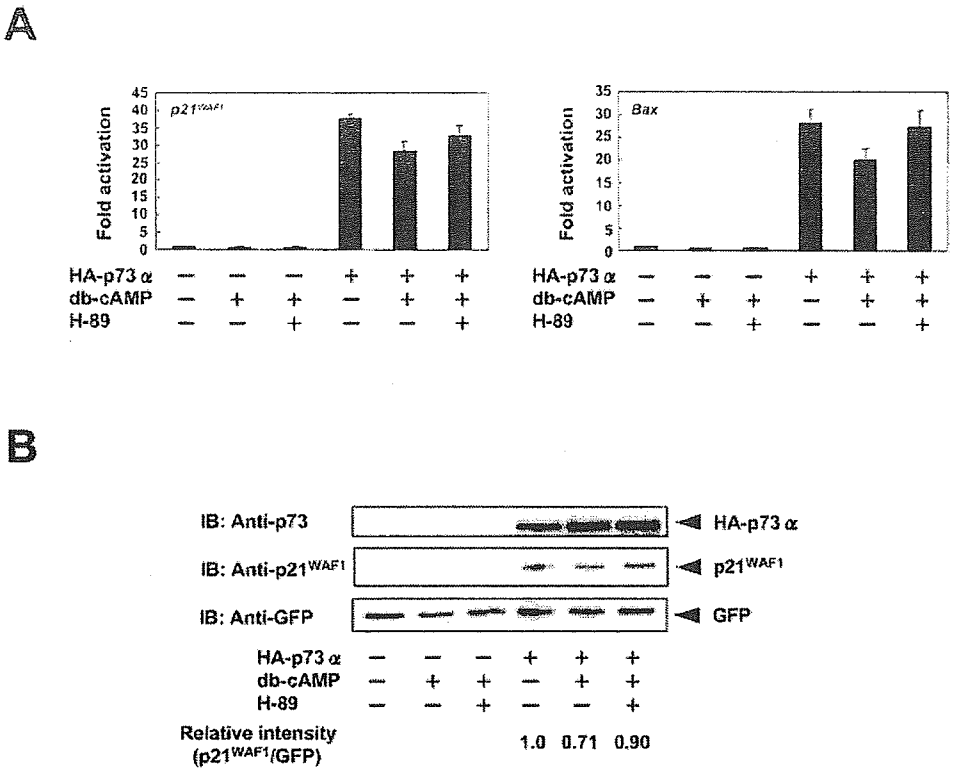

FIG. 7. **Effects of Bt_2cAMP on p73α-mediated transcriptional activation.** *A*, luciferase reporter analysis. H1299 cells were transiently cotransfected with 25 ng of the expression plasmid for HA-p73α, 100 ng of the luciferase reporter construct containing the p53/p73-responsive element derived from the $p21^{WAF1}$ (*left panel*) or *bax* (*right panel*) promoter, and 10 ng of pRL-TK. Twenty-four hours after transfection, cells were left untreated or were treated with Bt_2cAMP (*db-cAMP*; 1 mM) or with Bt_2cAMP (1 mM) plus the PKA inhibitor H-89 (10 μM) for 24 h. Cell lysates were then prepared and subjected to the determination of luciferase activity as described in the legend to Fig. 4. *B*, immunoblot analysis for $p21^{WAF1}$. H1299 cells were transiently cotransfected with 200 ng of the expression plasmid for HA-p73α and 50 ng of the GFP expression plasmid. Twenty-four hours after transfection, cells were treated with or without Bt_2cAMP (1 mM) in the presence or absence of H-89 (10 μM) for 24 h. Whole cell lysates were then prepared and subjected to immunoblotting (*IB*) with the indicated antibodies. Densitometry was used to quantify the amounts of $p21^{WAF1}$, which were normalized to GFP.

reduce the transcriptional activity of p73α, suggesting that the kinase activity of PKA-Cβ is required for its inhibitory effect on p73α. In accordance with these results, the transient activation of the cAMP/PKA signaling pathway by Bt_2cAMP reduced p73α-mediated transcriptional activation, whereas the inhibitory effect of Bt_2cAMP was attenuated when cells were exposed to H-89, a specific pharmacological inhibitor of PKA. Collectively, our present findings indicate that the PKA-mediated phosphorylation and conformational alteration of p73α might be a novel inhibitory mechanism of its activity.

As described previously (38), the PKA catalytic subunit family is composed of three isoforms: PKA-Cα, PKA-Cβ, and PKA-Cγ. PKA-Cα is expressed ubiquitously, whereas PKA-Cβ is expressed predominantly in brain and reproductive tissues (31, 32). PKA-Cβ is expressed as at least six variants (Cβ1, Cβ2, Cβ3, Cβ4, Cβ4ab, and Cβ4abc) arising from alternative splicing of the primary transcript (39). These splice variants contain a unique N terminus, but share a common catalytic domain, suggesting that they have similar enzymatic activity. Sequence analysis revealed that the PKA-Cβ we identified in this study is PKA-Cβ4ab. According to our *in vitro* phosphorylation assay using various truncated forms of GST-p73α as substrates, the N-terminal region of p73α (residues 1–130) might contribute to phosphorylation by PKA. As described previously (40, 41), the amino acid sequence (R/K)*XX*(S/T) is a consensus motif for PKA-dependent phosphorylation. Examination of the amino acid sequence of p73α for a putative PKA recognition site(s) showed three related motifs (^{78}RAAS^{81}, ^{164}KVST^{167}, and ^{402}KLPS^{405}). Ser-81 exists in the N-terminal region of p73α. It is thus likely that this site could be one of the site(s) phosphorylated by PKA, although there is no direct evidence for this possibility. Because PKA-Cβ(K76R), which retained the ability to bind to p73α, failed to inhibit p73α-mediated transcriptional activation, it is conceivable that the PKA-dependent phosphorylation of p73α might serve to modulate its function. Accumulating evidence suggests that, as for p53, post-translational modifications such as phosphorylation and acetylation regulate p73. In response to DNA-damaging agents, p73 is phosphorylated at Tyr-99, Ser-289, and Ser-47 by c-Abl, the protein kinase Cδ catalytic fragment, and Chk1, respectively (16–19, 25). Each of these phosphorylations is associated with the activation of p73. Alternatively, Pin1 recognizes phosphorylated Ser-412, Thr-442, and/or Thr-482 of p73, thereby activating p73 in association with the enhanced levels of its acetylation mediated by p300 (28). On the other hand, cyclin-dependent protein kinase-dependent phosphorylation of p73 at Thr-86 results in a significant reduction of the transcriptional activity of p73 (42). Accordingly, the identification of the precise phosphorylation site(s) of p73α by PKA is necessary to confirm the functional significance of the PKA-mediated phosphorylation of p73α.

We (36) and others (7, 43) reported that p73α exhibits a low level of transactivation ability relative to that of p73β, suggesting that the C-terminal extension of p73α exerts an inhibitory effect on the transcriptional activity of p73. Another p53 family member (p63) also showed similar results (44). Intriguingly, three-dimensional analysis demonstrated that the C-terminal region of p53 exists in close proximity to the central DNA-binding domain (45). In addition, it has been shown that the C

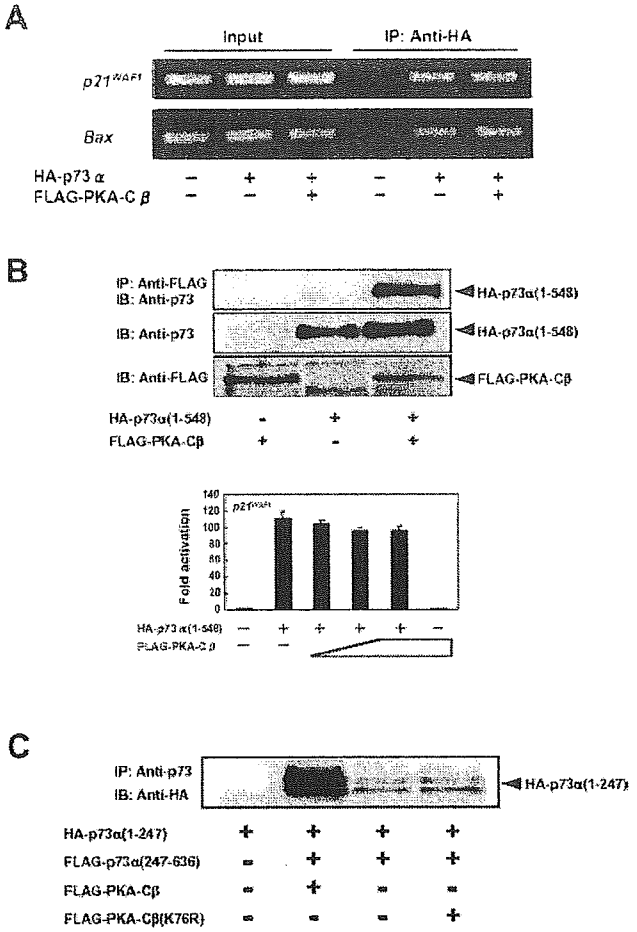

FIG. 8. **PKA-Cβ-mediated intramolecular interaction of p73α contributes to the down-regulation of the transcriptional activity of p73α.** *A*, ChIP assay. H1299 cells were transiently cotransfected with the expression plasmid for HA-p73α or HA-p73α plus FLAG-PKA-Cβ. Thirty-six hours after transfection, cells were fixed in formaldehyde and lysed, and DNA was sheared into 200–500-bp fragments by sonication. HA-p73α-bound DNA was immunoprecipitated (*IP*) with anti-HA monoclonal antibody. The amounts of HA-p73α bound to the p53/p73-responsive element within the $p21^{WAF1}$ (*upper panel*) or *bax* (*lower panel*) promoter region were analyzed by standard PCR. *B*, PKA-Cβ fails to inhibit p73α-(1–548). COS-7 cells were transiently cotransfected with the indicated combinations of expression plasmids. Forty-eight hours after transfection, whole cell lysates were prepared and subjected to co-immunoprecipitation (*first panel*) or immunoblotting (*second* and *third panels*) (*upper panels*). H1299 cells were transiently cotransfected with 25 ng of the expression plasmid for HA-p73α-(1–548), 100 ng of the luciferase reporter construct carrying the p53/p73-responsive element of the $p21^{WAF1}$ promoter, and 10 ng of pRL-TK with or without increasing amounts of the expression plasmid for FLAG-PKA-Cβ (25, 50, and 100 ng). Forty-eight hours after transfection, luciferase activity was determined as described in the legend to Fig. 4 (*lower panel*). *C*, the intramolecular interaction of p73α is stimulated by PKA-Cβ. Whole cell lysates prepared from COS-7 cells transfected with the indicated combinations of expression plasmids were immunoprecipitated with anti-p73 antibody, followed by immunoblotting (*IB*) with anti-HA antibody.

terminus of p53 directly interacts with and masks its DNA-binding domain, thereby inhibiting its DNA binding activity (46, 47). Recently, Serber *et al.* (37) found that the transcriptional activity of p63α is significantly inhibited by an intramolecular interaction. In sharp contrast to p53, the extreme C-terminal region of p63α binds to the N-terminal transactivation domain, but not to the DNA-binding domain, and abrogates its transactivation potential. Given the high amino acid sequence homology between p73α and p63α and their similar domain structure, the transcriptional activity of p73 might be regulated at least in part by an intramolecular inhibitory interaction. According to our *in vitro* pull-down assay, PKA-Cβ bound to the N- and C-terminal regions of p73α. Furthermore, the co-immunoprecipitation experiments demonstrated that p73α-(1–247) efficiently coprecipitated with p73α-(247–636) in the presence of PKA-Cβ, suggesting that PKA-Cβ might promote the intramolecular interaction of p73α to mask the N-terminal transactivation domain rather than the central DNA-binding domain and keep it in an inactive form. Indeed, our ChIP experiments revealed that PKA-Cβ had no significant effect on the DNA binding activity of p73α. Because the kinase-deficient mutant of PKA-Cβ failed to bridge p73α-(1–247) and p73α-(247–636), it is likely that the PKA-mediated phosphorylation of p73 plays an important role in the conformational alteration of p73. However, the precise molecular mechanism by which PKA-mediated phosphorylation could contribute to the inhibition of p73 is currently unknown.

It has been shown previously (48–50) that the activation of PKA has either mitogenic or anti-proliferative effects in mammalian cultured cells and that these opposite responses might be due to the existence of cell type-specific targets of this signaling pathway. Accumulating evidence indicates that the anti-apoptotic effect of PKA might be mediated by the activation of the ERK (extracellular signal-regulated kinase) (51, 52) and phosphatidylinositol 3-kinase/Akt (53, 54) pathways. Recently, Wu *et al.* (55) found that c-Myc enhances the activity of PKA by transactivating the expression of PKA-Cβ. According to their results, constitutive expression of PKA-Cβ results in the promotion of colony formation in soft agar medium, and PKA-Cβ- as well as c-Myc-mediated cellular transformation is markedly inhibited by H-89, suggesting that PKA might be one of the downstream mediators of c-Myc function. As described previously (55–57), PKA directly phosphorylates Bad and glycogen synthase kinase-3β to inhibit their apoptosis-inducing activity. Likewise, our present findings indicate that the PKA-mediated phosphorylation of pro-apoptotic p73 abrogates its function. Thus, it is likely that the anti-apoptotic function of PKA is at least in part due to the inactivation of p73 and the subsequent suppression of apoptotic signaling.

Acknowledgments—We thank members of our laboratory for stimulating discussions and Yuki Nakamura for excellent technical assistance.

REFERENCES

1. Kaghad, M., Bonnet, H., Yang, A., Creancier, L., Biscan, J. C., Valent, A., Minty, A., Chalon, P., Lelias, J. M., Dumont, X., Ferrara, P., McKeon, F., and Caput, D. (1997) *Cell* **90,** 809–819
2. Jost, C. A., Marin, M. C., and Kaelin, W. G., Jr. (1997) *Nature* **389,** 191–194
3. De Laurenzi, V., Costanzo, A., Barcaroli, D., Torrinoni, A., Falcico, M., Annicchiarico-Petruzzelli, M., Levrero, M., and Melino, G. (1998) *J. Exp. Med.* **188,** 1763–1768
4. Di Como, C. J., Gaiddon, C., and Prives, C. (1999) *Mol. Cell. Biol.* **19,** 1438–1449
5. Steegenga, W. T., Shvarts, A., Riteco, N., Bos, J. L., and Jochemsen, A. G. (1999) *Mol. Cell. Biol.* **19,** 3885–3894
6. Zeng, X., Chen, L., Jost, C. A., Maya, R., Keller, D., Wang, X., Kaelin, W. G., Jr., Oren, M., Chen, J., and Lu, H. (1999) *Mol. Cell. Biol.* **19,** 3257–3266
7. Ueda, Y., Hijikata, M., Takagi, S., Chiba, T., and Shimotohno, K. (1999) *Oncogene* **18,** 4993–4998
8. De Laurenzi, V., Catani, M. V., Teminoni, A., Corazzari, M., Melino, G., Costanzo, A., Levrero, M., and Knight, R. A. (1999) *Cell Death Differ.* **6,** 389–390
9. Ishimoto, O., Kawahara, C., Enjo, K., Obinata, M., Nukiwa, T., and Ikawa, S. (2002) *Cancer Res.* **62,** 636–641
10. Yang, A., Walker, N., Bronson, R., Kaghad, M., Oosterwegel, M., Bonnin, J., Vagner, C., Bonnet, H., Dikkens, P., Sharpe, A., McKeon, F., and Caput, D. (2000) *Nature* **404,** 99–103
11. Pozniak, C. D., Radinovic, S., Yang, A., McKeon, F., Kaplan, D. R., and Miller, F. D. (2000) *Science* **289,** 304–306
12. Stiewe, T., Zimmermann, S., Frilling, A., Esche, H., and Putzer, B. M. (2002) *Cancer Res.* **62,** 3598–3602
13. Grob, T. J., Novak, U., Maisse, C., Barcaroli, D., Luthi, A. U., Pirnia, F., Hugli, B., Graber, H. U., De Laurenzi, V., Fey, M. F., Melino, G., and Tobler, A. (2001) *Cell Death Differ.* **8,** 1213–1223
14. Nakagawa, T., Takahashi, M., Ozaki, T., Watanabe, K., Todo, S., Mizuguchi, H., Hayakawa, T., and Nakagawara, A. (2002) *Mol. Cell. Biol.* **22,** 2575–2585

15. Zaika, A. I., Slade, N., Erster, S. H., Sansome, C., Joseph, T. W., Pearl, M., Chalas, E., and Moll, U. M. (2002) *J. Exp. Med.* **196,** 765–780
16. Gong, J., Costanzo, A., Yang, H. Q., Melino, G., Kaelin, W. G., Jr., Levrero, M., and Wang, J. Y. (1999) *Nature* **399,** 806–809
17. Agami, R., Blandino, G., Oren, M., and Shaul, Y. (1999) *Nature* **399,** 809–813
18. Yuan, Z.-M., Shioya, H., Ishiko, T., Sun, X., Gu, J., Huang, Y. Y., Lu, H., Kharbanda, S., Weichselbaum, R., and Kufe, D. (1999) *Nature* **399,** 814–817
19. Ren, J., Datta, R., Shioya, H., Li, Y., Oki, E., Biedermann, V., Bharti, A., and Kufe, D. (2002) *J. Biol. Chem.* **277,** 33758–33765
20. Yuan, Z.-M., Utsugisawa, T., Ishiko, T., Nakada, S., Huang, Y., Kharbanda, S., Weichselbaum, R., and Kufe, D. (1998) *Oncogene* **16,** 1643–1648
21. Sun, X., Wu, F., Datta, R., Kharbanda, S., and Kufe, D. (2000) *J. Biol. Chem.* **275,** 7470–7473
22. Sanchez, Y., Wong, S., Thoma, R. S., Richman, R., Wu, Z., Piwnica-Worms, H., and Elledge, S. J. (1997) *Science* **277,** 1497–1501
23. Liu, Q., Guntuku, S., Cui, X. S., Matsuoka, S., Cortez, D., Tamai, K., Luo, G., Carattini-Rivera, S., DeMaya, F., Bradley, A., Donehower, L. A., and Elledge, S. J. (2000) *Genes Dev.* **14,** 1448–1459
24. Zhao, H., and Piwnica-Worms, H. (2001) *Mol. Cell. Biol.* **21,** 4129–4139
25. Gonzalez, S., Prives, C., and Cordon-Cardo, C. (2003) *Mol. Cell. Biol.* **23,** 8161–8171
26. Zeng, X., Li, X., Miller, A., Yuan, Z., Yuan, W., Kwok, R. P., Goodman, R., and Lu, H. (2000) *Mol. Cell. Biol.* **20,** 1299–1310
27. Costanzo, A., Melro, P., Pediconi, N., Fulco, M., Sartorelli, V., Cole, P. A., Fontemaggi, G., Fanciulli, M., Schiltz, L., Blandino, G., Balsano, C., and Levrero, M. (2002) *Mol. Cell* **9,** 175–186
28. Mantovani, F., Piazza, S., Gostissa, M., Strano, S., Zacchi, P., Mantovani, R., Blandino, G., and Del Sal, G. (2004) *Mol. Cell* **14,** 625–636
29. Watanabe, K., Ozaki, T., Nakagawa, T., Miyazaki, K., Takahashi, M., Hosoda, M., Hayashi, S., Todo, S., and Nakagawara, A. (2002) *J. Biol. Chem.* **277,** 15113–15123
30. Nakamura, Y., Ozaki, T., Nakagawara, A., and Sakiyama, S. (1997) *Eur. J. Cancer* **33,** 1986–1990
31. Uhler, M. D., Chrivia, J. C., and McKnight, G. S. (1986) *J. Biol. Chem.* **261,** 15360–15463
32. Cadd, G., and McKnight, G. S. (1989) *Neuron* **3,** 71–79
33. Taylor, S. S., Buechler, J. A., and Yenemoto, W. (1990) *Annu. Rev. Biochem.* **59,** 971–1005
34. Scott, J. D. (1991) *Pharmacol. Ther.* **50,** 123–145
35. Irwin, M. S., Kondo, K., Marin, M. C., Cheng, L. S., Hahn, W. C., and Kaelin, W. G., Jr. (2003) *Cancer Cells* **3,** 403–410
36. Ozaki, T., Naka, M., Takada, N., Tada, M., Sakiyama, S., and Nakagawara, A. (1999) *Cancer Res.* **59,** 5902–5907
37. Serber, Z., Lai, H. C., Yang, A., Ou, H. D., Sigal, M. S., Kelly, A. E., Darimont, B. D., Duijf, P. H. G., van Bokhoven, H., McKeon, F., and Dotsch, V. (2002) *Mol. Cell. Biol.* **22,** 8601–8611
38. Skalhegg, B. S., and Tasken, K. (2000) *Front. Biosci.* **5,** 678–693
39. Ørstavik, S., Reinton, N., Frengen, E., Langeland, B. T., Jahnsen, T., and Skalhegg, B. S. (2001) *Eur. J. Biochem.* **268,** 5066–5073
40. Kemp, B. E., Graves, D. J., Benjamin, E., and Krebs, E. G. (1977) *J. Biol. Chem.* **252,** 4888–4894
41. Higuchi, H., Yamashita, T., Yoshikawa, H., and Tohyama, M. (2003) *EMBO J.* **22,** 1790–1800
42. Gaiddon, C., Lokshin, M., Gross, I., Levasseur, D., Taya, Y., Loeffler, J.-P., and Prives, C. (2003) *J. Biol. Chem.* **278,** 27421–27431
43. Lee, C.-W., and La Thangue, N. B. (1999) *Oncogene* **18,** 4171–4181
44. Yang, A., and McKeon, F. (2000) *Nat. Rev. Mol. Cell. Biol.* **1,** 199–207
45. Friend, S. (1994) *Science* **265,** 334–335
46. Hupp, T. R., and Lane, D. P. (1994) *Cold Spring Harbor Symp. Quant. Biol.* **59,** 195–206
47. Hupp, T. R., Sparks, A., and Lane, D. P. (1995) *Cell* **83,** 237–245
48. Smets, L. A., and Van Rooy, H. (1987) *J. Cell. Physiol.* **133,** 395–399
49. Zachary, I., Masters, S. B., and Bourne, H. R. (1990) *Biochem. Biophys. Res. Commun.* **168,** 1184–1193
50. Chen, J., and Iyengar, R. (1994) *Science* **263,** 1278–1281
51. Xia, Z., Dickens, M., Raingeaud, J., Davis, R. J., and Greenberg, M. E. (1995) *Science* **270,** 1326–1331
52. Anderson, C. N., and Tolkovsky, A. M. (1999) *J. Neurosci.* **19,** 664–673
53. Sable, C. L., Filippa, N., Hemmings, B., and Van Obberghen, E. (1997) *FEBS Lett.* **409,** 253–257
54. Filippa, M., Sable, C. L., Filloux, C., Hemmings, B., and Van Obberghen, E. (1999) *Mol. Cell. Biol.* **19,** 4989–5000
55. Wu, K.-J., Mattioli, M. M., Morse, H. C., III, and Dalla-Favera, R. (2002) *Oncogene* **21,** 7872–7882
56. Harada, H., Becknell, B., Wilm, M., Mann, M., Huang, L. J.-S., Taylor, S. S., Scott, J. D., and Korsmeyer, S .J. (1999) *Mol. Cell* **3,** 413–422
57. Li, M., Wang, X., Meintzer, M. K., Laessig, T., Birnbaum, M. J., and Heidenreich, K. A. (2000) *Mol. Cell. Biol.* **20,** 9356–9363

FEBS Letters 580 (2006) 627–632

High expression of *N*-acetylglucosaminyltransferase V in favorable neuroblastomas: Involvement of its effect on apoptosis

Kei-ichiro Inamori[a], Jianguo Gu[a,*], Miki Ohira[b], Atsushi Kawasaki[b], Yohko Nakamura[b], Takatoshi Nakagawa[c], Akihiro Kondo[c], Eiji Miyoshi[a], Akira Nakagawara[b], Naoyuki Taniguchi[a]

[a] *Department of Biochemistry, Osaka University Graduate School of Medicine, 2-2 Yamadaoka, Suita, Osaka 565-0871, Japan*
[b] *Division of Biochemistry, Chiba Cancer Center Research Institute, 666-2 Nitona, Chuoh-ku, Chiba 260-8717, Japan*
[c] *Department of Glycotherapeutics, Osaka University Graduate School of Medicine, 2-2 Yamadaoka, Suita, Osaka 565-0871, Japan*

Received 1 December 2005; revised 27 December 2005; accepted 29 December 2005

Available online 5 January 2006

Edited by Laszlo Nagy

Abstract **Neuroblastoma (NBL), derived from the sympathetic precursor cells, is one of the most common pediatric solid tumors. The expression of *N*-acetylglucosaminyltransferase V and IX (GnT-V and GnT-IX) mRNA in 126 primary NBLs were quantitatively analyzed and higher expression levels of GnT-V were found to be associated with favorable stages (1, 2 and 4s). Conversely, the downregulation of GnT-V expression by small interfering RNA resulted in a decrease in the susceptibility to cell apoptosis induced by retinoic acid in NBL cells accompanied by morphological change. These results suggest that GnT-V is associated with prognosis by modulating the sensitivity of NBLs to apoptosis.**

Keywords: Neuroblastoma; GnT-V; GnT-IX; Retinoic acid; Apoptosis

1. Introduction

Aberrant glycosylation occurs in nearly all types of cancers, and has been implicated in the malignancy that is characteristic of the disease [1]. *N*-acetylglucosaminyltransferase V (GnT-V) is one of the most relevant glycosyltransferases to tumor invasion and metastasis, and catalyzes the formation of β1,6GlcNAc branching on *N*-glycans, which is closely associated with malignant transformations [2–6]. Recently, our group and Pierce's group independently reported on a new *N*-acetylglucosaminyltransferase IX (GnT-IX, also referred to as GnT-VB), a GnT-V homolog, that is specifically expressed in the brain [7,8]. GnT-IX transcripts are exclusively expressed in the brain and testis, while GnT-V is expressed ubiquitously in human and mouse tissues. Since both glycosyltransferases are expressed in the mouse brain in a region-specific manner (unpublished data), it is possible that they may have discrete biological functions in the brain. On the other hand, GnT-V and GnT-IX are both highly expressed in both the adult and fetal brain [7,9], as well as in several human neuroblastoma (NBL) cell lines (this study and unpublished data). This prompted us to examine the expression of GnT-V and GnT-IX in primary NBL tissues.

NBL is a tumor derived from primitive cells of the sympathetic nervous system and is the most common solid tumor in childhood [10]. Interestingly, most NBLs in infants regress spontaneously or mature into a benign ganglioneuroma. These tumors usually express high levels of TrkA, and as a result, have a tendency to either undergo apoptosis or differentiation, depending on whether nerve growth factor is present or absent in their microenvironment. On the other hand, in most patients over 1 year of age who have metastatic disease, the tumor grows aggressively and their prognosis is usually poor.

In this study, we carried out a quantitative analysis of the gene expression of these glycosyltransferases by real-time PCR, and the findings indicate that a higher expression of GnT-V is correlated with a favorable prognosis for NBL patients. Furthermore, to explore the underlying molecular mechanism, we devised a knockdown approach, in which small interfering RNA (siRNA)-directed against GnT-V mRNA was used to investigate the susceptibility to cell apoptosis induced by retinoic acid in NBL cells. The results clearly showed that the expression levels of GnT-V are associated with a favorable prognosis, possibly through sensitizing to apoptotic signals.

2. Materials and methods

2.1. RNA isolation from primary NBLs

Fresh, frozen tumor tissues were sent to the Division of Biochemistry, Chiba Cancer Center Research Institute, from various hospitals in Japan with informed consent from the patients' parents. All samples were obtained by surgery or biopsy and had been stored at 80 °C. The RNA samples obtained from 126 patients with NBL were subjected to semiquantitative and quantitative real-time reverse transcription-PCR (RT-PCR) analyses. All of the patients were diagnosed clinically as well as pathologically and were tested for DNA ploidy, MYCN amplification, and TrkA expression. The tumors were staged according to the criteria of the International Neuroblastoma Staging System [11].

2.2. Semiquantitative RT-PCR analysis of primary NBLs

The preparation of total RNA from NBL tissues and the synthesis of the first-strand cDNA were performed as described previously [12]. The cDNA was diluted to a 1:20 solution and then amplified in a final

*Corresponding author. Fax: +81 6 6879 3429.
E-mail address: jgu@biochem.med.osaka-u.ac.jp (J. Gu).

Abbreviations: NBL, neuroblastoma; GnT-V, *N*-acetylglucosaminyltransferase V; GnT-IX, *N*-acetylglucosaminyltransferase IX; RT, reverse transcription; PARP, poly(ADP-ribose) polymerase

0014-5793/$32.00
doi:10.1016/j.febslet.2005.12.089

volume of 10 μl of reaction mixture containing 200 μM of dNTPs, 1× PCR buffer, 0.5 μM of each primer and 0.2 U of rTaq DNA polymerase (Takara Bio, Ohtsu, Japan). The following primer sets were used: GnT-V, 5′-GACCTGCAGTTCCTTCTTCG-3′ and 5′-CCATGGCAGAAGTCCTGTTT-3′; GnT-IX, 5′-CATGGCACCGTGTACTAC-3′ and 5′-TCTGGAGCTCTGCAGAAG-3′. PCR templates were standardized by their GAPDH expression before performing the RT-PCR experiments.

2.3. Quantitative real-time PCR analysis of primary NBLs

2 μl of cDNA prepared as above, either a 100-fold dilution for GnT-V or a 20-fold dilution for GnT-IX, was amplified in a volume of 20 μl with Assay-on-Demand Gene Expression Products (Applied Biosystems) consisting of primers and a TaqMan probe (Assay ID: GnT-V, Hs00159136_m1; GnT-IX, Hs01586304_g1). The thermal cycling conditions and the normalization of the data using GAPDH expression were performed as described previously [12]. All experiments were carried out in triplicate for each data point.

2.4. Assay of GlcNAc transferase activity

The activities of GnT-V and GnT-III in whole cell lysates or microsomal fractions were determined using a pyridylaminated biantennary sugar chain as an acceptor substrate, as described previously [7,13].

2.5. Construction of siRNA vector and retroviral infection

Small interfering oligonucleotides specific for GnT-V were designed on the Takara Bio website (http://www.takara-bio.co.jp/) and the oligonucleotide sequences used in the construction of the siRNA vector were as follows: 5′-GATCCGTTCATTGGCGGAAATTCGTTTCAAGAGAACGAATTTCCGCCAATGAACTTTTTTAT-3′ and 5′-CGATAAAAAAGTTCATTGGCGGAAATTCGTTCTCTTGAAACGAATTTCCGCCAATGAACG-3′. The oligonucleotides were annealed and then ligated into *Bam*HI/*Cla*I sites of the pSINsi-hU6 vector (Takara Bio). A retroviral supernatant was obtained by transfection of human embryonic kidney 293 cells using a Retrovirus Packaging Kit Ampho (Takara Bio) according to the manufacturer's protocol. CHP134 cells, a human NBL cell line, were infected with the viral supernatant, and the cells were then selected with 0.5 mg/ml G418 for 2–3 weeks. Stable GnT-V-knockdown clones were selected and confirmed by GnT-V activity and gene expression. Quantitative real-time PCR analyses of GnT-V mRNA expression in these clones were performed with a Smart Cycler II System and the SYBR premix Taq (Takara Bio). RT was carried out at 42 °C for 10 min, followed by 95 °C for 2 min using random primers, followed by PCR for 50 cycles at 95 °C for 5 s and 60 °C for 20 s with the following primers: 5′-AAGCAGGTGTGCCAGGAGAG-3′ and 5′-GTCAAAGGAGGGCACCAGGA-3′. Normalization of the data was performed using the GAPDH mRNA levels.

2.6. Analysis of retinoic acid-induced apoptosis

Parent, mock, and GnT-V-knockdown CHP134 cells were plated on 10 cm culture dishes at 5×10^5 cells in RPMI1640 supplemented with 10% fetal bovine serum, 100 U/ml penicillin, and 0.1 mg/ml streptomycin. After incubation for 24 h, the conditioned media were changed with fresh medium containing various concentrations of all-*trans* retinoic acid (Sigma). The cells were washed twice with PBS and harvested at the indicated times. Retinoic acid-induced apoptosis was estimated by detecting the cleavage of poly ADP-ribose polymerase (PARP) in whole cell lysates by Western blot analysis using a human specific anti-cleaved PARP (Asp214) antibody (Cell Signaling Technology). As a loading control, anti-ERK1/2 (p44/42 MAP Kinase Antibody, Cell Signaling Technology) was used.

2.7. Viability assay of retinoic acid-treated cells

The parent, mock, and GnT-V-knockdown CHP134 cells were seeded on a 96-well plate at 3×10^3 cells/well for 24 h prior to the retinoic acid treatment. The cells were then incubated with or without retinoic acid at the indicated concentrations for 3 days. Cell viability was assayed using a Cell Counting Kit-8 (Dojindo, Kumamoto, Japan) according to the manufacture's instructions. All experiments were carried out in triplicate for each data point.

3. Results

3.1. Association between higher expression levels of GnT-V mRNA and favorable prognosis in primary NBLs

To assess the association between GnT-V or GnT-IX mRNA expression and the prognosis of the NBLs, we first performed semiquantitative RT-PCR analyses using 16 favorable and 16 unfavorable NBLs. As shown in Fig. 1, GnT-V was preferentially expressed in most of the favorable NBLs, while no obvious difference in GnT-IX expression was found between favorable and unfavorable NBLs. Table 1 shows quantitative data for GnT-V and GnT-IX mRNA in 126 primary NBLs with tumor stages (1, 2, 4s versus 3, 4). GnT-V expression was significantly increased in NBLs at favorable stages ($P = 0.021$), and was correlated well with higher expression of TrkA ($P = 0.010$). On the other hand, GnT-IX expression was marginally associated with the stages.

3.2. GnT-V activities in various human NBL cell lines

To determine whether the expression level of GnT-V is also increased in NBL cells, the activities of GnT-V in various human NBL cell lines were examined. As shown in Fig. 2A, each cell line expressed GnT-V activity at distinct levels. The CHP134 cells showed the highest GnT-V activity among the 10 NBL cell lines used in this study. It is known that the cell line is highly sensitive to the induction of apoptosis by all-*trans* retinoic acid [14,15]. In fact, it is thought that favorable NBLs usually express higher levels of TrkA, and tend to regress spontaneously due to apoptosis. As shown in Fig. 2B, in CHP134 cells that had been treated with retinoic acid at a concentration of 1 μM or 5 μM, PARP cleavage, a marker for apoptosis, occurred, which is one of the main cleavage targets of caspase-3

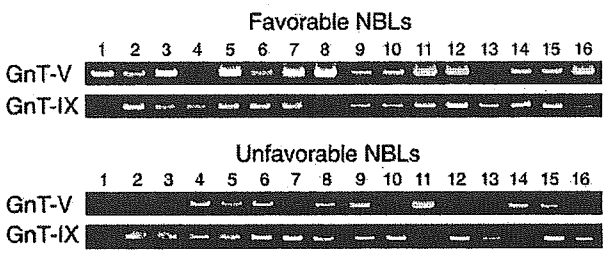

Fig. 1. Semiquantitative RT-PCR analysis of favorable and unfavorable subsets of NBL. Sixteen favorable cases were in stage 1 with no MYCN amplification and a high TrkA expression, while 16 unfavorable cases were in stage 3 or 4 with MYCN amplification and a low TrkA expression.

Table 1
Association of tumor stages and *TrkA* expression in NBL patients with GnT-V or GnT-IX mRNA expression levels

	n	GnT-V[a]	*P*	GnT-IX[a]	*P*
Tumor stage					
1, 2, 4s	57	2.23 ± 0.29	0.021	1.78 ± 0.25	0.21
3, 4	69	1.48 ± 0.16		2.23 ± 0.25	
TrkA expression					
High	59	2.11 ± 0.27	0.010	1.86 ± 0.17	0.75
Low	48	1.33 ± 0.13		1.98 ± 0.34	

[a]Means ± S.E.M.